Laboratory, Lexington, KY, 1:2,000), vimentin (Zymed, 1:100), and ubiquitin (Dako, Carpenteria, CA, 1:400). For controls, the primary antibody was replaced with normal rabbit serum or was omitted (these controls always yielded negative staining). For immunofluorescence studies, secondary antibodies were anti-mouse-Cy3 or -FITC or anti-rabbit-conjugated-Cy3 or -FITC (Jackson ImmunoResearch, West Grove, PA, 1:500).

TUNEL Assay

TUNEL staining was performed according to the original protocol, with modifications (Harada et al., 2004). The number of apoptotic cells was determined by counting positively stained nuclei in 30 tubule cross-sections per testis section in each testis (Kwon et al., 2004b). For clarity and brevity, we also counted all the TUNEL-stained cells within the entire cell population of testicular tubules in each section. In addition, we also counted the apoptosis-positive tubules (i.e., tubules containing at least one apoptotic cell) in each testis.

Western Blotting

Protein lysates were prepared from mouse testes as described (Kwon et al., 2004b). Approximately 20 μg of total protein was loaded per lane on 15% SDS–PAGE gels. Primary antibodies (diluted as indicated) were used to detect the following proteins: UCH-L1 (RA95101, 1:5,000), FLAG (FM2, Sigma, 1:2,000), Bcl-2 (Cell Signaling, Beverly, MA, 1:1,000), caspase-3 (Cell Signaling, 1:400), polyubiquitin (FK2 clone, Medical & Biological Laboratory, Nagoya, Japan, 1:1,000), and monoubiquitin (U5379, Sigma, 1:1,000). Blots were further incubated with peroxidase-conjugated goat anti-mouse IgG or goat anti-rabbit IgG (1:5,000; Pierce, Rockford, IL) for 1 hr at room temperature. Immunoreactions were visualized using the SuperSignal West Dura extended duration substrate (Pierce) and analyzed with a ChemiImager (Alpha Innotech, San Leandro, CA). ChemiImager data were analyzed using AlphaEase software (Alpha Innotech) to yield the relative level of each protein.

RESULTS

Sterile Phenotype of *Uchl1* Tg Mice

We initially attempted to overexpress *Uchl1* in neurons using a Tg construct containing the *EF-1α* promoter (Mizushima and Nagata, 1990). The transgene was also strongly expressed in gonads as well as other Tg mice via the same promoter (Furuchi et al., 1996). We obtained six Tg mice having high transgene copy number, each of which most likely carried the transgene in a unique genomic location (see below). Four of these mice were females (Tg11, Tg12, Tg43, Tg81) and two were males (Tg21 and Tg22). Unexpectedly, all of these Tgs were sterile. Thus, it was not possible to maintain Tg lines during the course of these experiments. However, in addition to the sterile phenotype, the six independent Tg mice showed a similar pattern of *Uchl1* transgene expression and common pathological defects, the latter being limited to the testes or ovaries. The Tg loci were generated by random integration rather than by site-specific recombination, and thus the animals produced by our Tg procedure usually had more than one transgene integrated at each chromosomal site (Kroll and Amaya, 1996). Therefore, in each of the six Tg mice, the transgene most likely integrated into a different genomic site, raising the possibility of different position-dependent effects. Our data showed that we obtained multiple animals with similar patterns or levels of *Uchl1* transgene expression and with common pathological defects, suggesting the phenotypes reflect position-independent expression (i.e., independent of the position of transgene insertion). Thus, these Tg mice had similar infertile phenotypes that may be attributed to the overproduction of UCH-L1. Numerous gene inactivation studies have identified gene products involved in male fertility, but in most cases female reproduction was unaffected or weak damaged (Yuan et al., 2000). However, both male and female *Uchl1* Tg mice were infertile, although there were clear differences in germinal cell maturation, suggesting that UCH-L1 is required for both spermatogenesis and oogenesis. Therefore, six independent Tg founders, notably two males (Tg21 and Tg22), were analyzed in our present study.

The mating of two heterozygous Tg males with non-Tg females did not yield offspring until the age of 6 months, despite grossly normal appearance. This was also the case for the mating of four heterozygous Tg females with non-Tg males. Their non-Tg littermates sired offspring normally. At autopsy, the testes of both Tg21 and Tg22 appeared grossly smaller than those of non-Tg mice. The testes weight of Tg21 (77 mg) and Tg22 (70 mg) was only 42% and 38%, respectively, relative to non-Tg males (183 ± 16 mg), demonstrating that mice overexpressing UCH-L1 display profoundly defective testis development.

Expression Levels of the *Uchl1* Transgene

We used RT-PCR and primers specific for the *Uchl1* transgene to compare transgene expression levels in the testes or ovaries of the six Tg mice. There was some variation between animals (Fig. 1A). All the Tgs expressed a similar level of endogenous *Uchl1* mRNA (Fig. 1A); quantitation of absolute Tg *Uchl1* copy numbers using real-time quantitative RT-PCR showed that all six Tgs expressed 2.9–6.8-fold more *Uchl1* transgene mRNA compared with endogenous mRNA (4.5, 3.6, 6.2, 3.7, 2.9, and 6.8 for Tg21, Tg22, Tg11, Tg12, Tg43, and Tg81, respectively). Relative UCH-L1 protein expression was similar among four of the Tgs (76.1 ± 5.2; Fig. 1B) but was somewhat higher in Tg 21 (100) and Tg81 (106.2). The average level of endogenous UCH-L1 expression in Tg mice was ~91% relative to non-Tg mice (Fig. 1B).

Immunohistochemistry of testicular sections using an antibody against FLAG revealed that exogenous UCH-L1 localized mainly in spermatogonia and Sertoli cells (Fig. 2E), similar to the localization of endogenous UCH-L1 (Fig. 2A). Endogenous UCH-L1 localized to both the cytoplasm and nucleus of spermatogonia and Sertoli

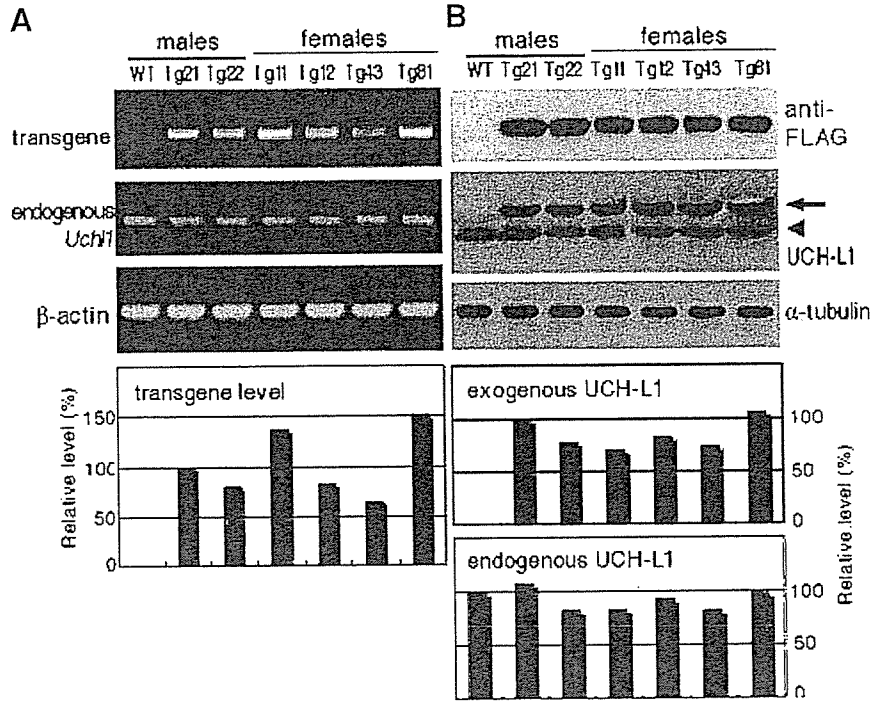

Fig. 1. Expression of transgenic ubiquitin carboxyl-terminal hydrolase 1 (UCH-L1) in the testes of Tg21 and Tg22 male mice. **A**: Transgenic *Uchl1* mRNA levels in the testes. RT-PCR showed high levels of *Uchl1* transgene mRNA in both Tg21 and Tg22 as well as in all ovaries from four female Tg mice. All Tg mice had a normal level of endogenous *Uchl1* mRNA. The relative expression level is indicated below each lane (as a percentage, scaled to β-actin in each lane). **B**: Western blot analysis of testicular or ovarian lysates. Both endogenous and exogenous UCH-L1 were detected with anti-UCH-L1, whereas exogenous UCH-L1 was specifically detected by anti-FLAG. Exogenous UCH-L1 (arrow) is slightly larger than endogenous UCH-L1 (arrowhead). WT, non-Tg wild-type.

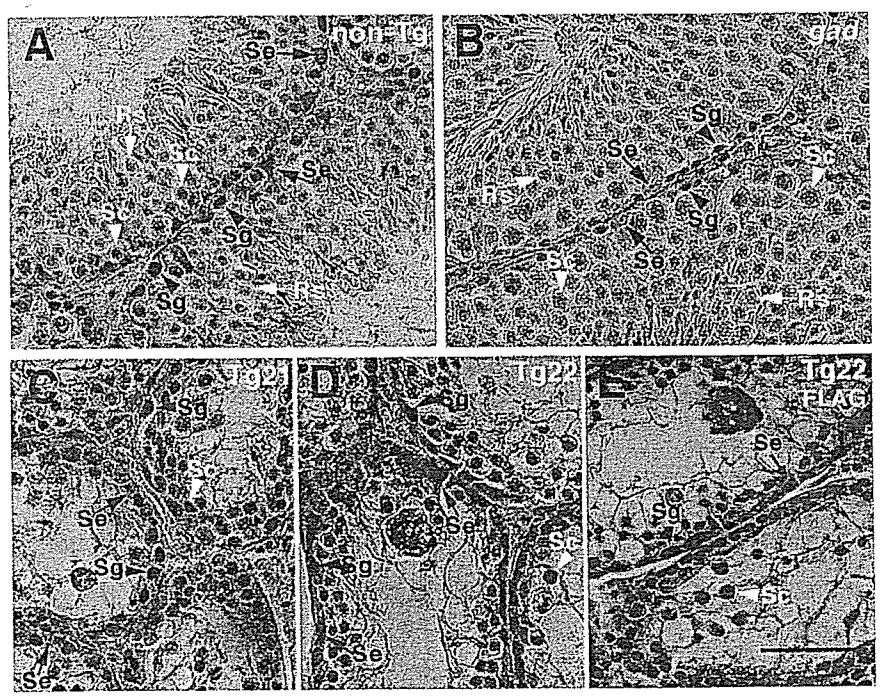

Fig. 2. Immunostaining of FLAG and UCH-L1 in *Uchl1* Tg mice shows high levels of UCH-L1 in testicular tubules. UCH-L1 immunostaining is clearly present in spermatogonia (Sg) and Sertoli cells (Se) of a non-Tg mouse (**A**) but not in a *gad* mouse (**B**). In contrast, in the testes of two Tg males, the most intense UCH-L1 immunoreactivity occurs predominantly in spermatogonia (Sg, arrowheads) and Sertoli cells (Se, arrows) but not in the primary spermatocytes (Sc, white arrowheads; **C**, Tg21; **D**, Tg22). **E**: Immunostaining of FLAG confirmed the transgene-derived UCH-L1 proteins in spermatogonia (Sg, arrowheads) and Sertoli cells (Se, arrows) but not in the primary spermatocytes (Sc, white arrowheads; Tg22). Magnification: ×400. Scale bar, 50 μm.

cells in the testes of non-Tg males; however, localization was not apparent around pachytene spermatocytes or round, elongated spermatids (Fig. 2A). This distribution of UCH-L1 is in good agreement with previous reports (Kon et al., 1999; Kwon et al., 2004a). Compared with non-Tg males, overexpression of UCH-L1 in seminiferous tubules of Tg males (Tg21 and Tg22) occurred predominantly in spermatogonia and Sertoli cells, and was weakly positive or negative in spermatocytes (Fig. 2C,D). These data coincided with strong induction of the *Uchl1* transgene. Tg mice expressed a higher level of total UCH-L1 (both endogenous and exogenous), suggesting a correlation between excess UCH-L1 and sterility.

Morphological Examination

Histopathological analysis of testes from 6-month-old Tg21 and Tg22 revealed terminal loss of differentiated germ cells and a large number of pachytene spermatocytes that had degenerated (with condensed nuclei and giant cells) and been sloughed off, forcing an altered structure of the seminiferous tubules such that they appeared almost empty (Fig. 3A). The deformed seminiferous tubules also contained numerous arrested spermatocytes (Fig. 3A, arrowheads) and multinucleated giant cells (arrows). In contrast, the seminiferous tubules of *gad* mice were nearly intact, as in non-Tg males (data not shown). In non-Tg males, seminiferous tubules containing elongated spermatids in the inner layer were readily detected (data not shown), whereas these tubules were scarcely detectable in Tg21 (Fig. 3A) and Tg22. On the other hand, the four female Tg mice displayed a variety of phenotypes, including an increased number of apoptotic oocytes and granulosa cells relative to non-Tg females, leading to infertility (data not shown).

In non-Tg (Fig. 3B) and *gad* mice (Fig. 3C), only a few TUNEL-positive cells were identified, located at the periphery of the tubule. However, many fewer TUNEL-positive cells were detected in the Tg males (Fig. 3D,E), and cell morphology indicated that most of these positive cells were primary spermatocytes. However, neither the TUNEL assay nor microscopy revealed evidence of apoptosis in spermatogonia or Sertoli cells. We quantitatively assessed germ cell apoptosis in Tg, non-Tg, and *gad* mice by calculating the number of apoptotic cells per tubules in each testis. This value was 25 times higher in Tg testes compared with non-Tg or *gad* testes (the averages $\pm$ SD were as follows: 553 ± 72, $n = 2$ in Tg testes; 22 ± 4.2, $n = 3$ in non-Tg; and 21 ± 5.3, $n = 3$ in *gad*). The percentage of apoptosis-positive tubules in Tg testes was also significantly higher than in non-Tg or *gad* mice (the averages $\pm$ SD were as follows: 95.3 ± 2.7, $n = 2$ in Tg testes; 7.4 ± 2.2, $n = 3$ in non-Tg; and 7.1 ± 1.8, $n = 3$ in *gad*).

A control section of caput epididymis, an androgen-dependent organ, from same Tg mice was investigated. No UCH-L1 overexpressing was detected, and no pathological symptoms could be observed in the epididymis (data not shown).

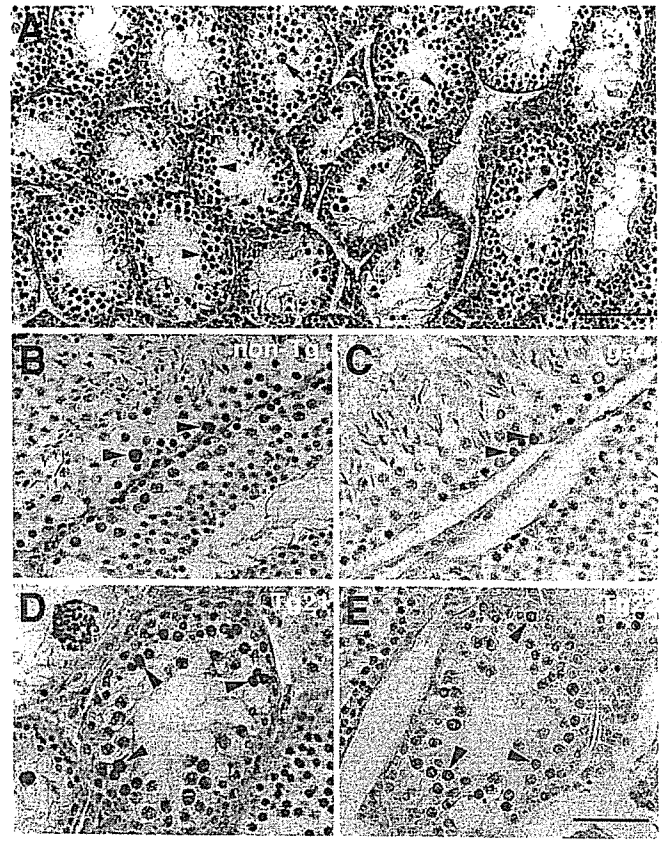

Fig. 3. Histopathology and TUNEL assay in situ. **A**: Hematoxylin–eosin staining of testis sections from the Tg21 male mouse shows defective spermatogenesis. Arrowheads indicate arrested spermatocytes and arrows indicate giant cells. Round spermatocytes and spermatids were rarely observed. **B–E**: Examples of TUNEL-positive cells characterized by the robust deposition of the reddish brown reaction product in sections of testis from non-Tg (B), *gad* (C), and Tg mice (D, Tg21; E, Tg22). Sections were counterstained with hematoxylin. A large number of TUNEL-positive cells were clearly observed at the periphery of the seminiferous tubule (arrowheads) in Tg21 (D) and Tg22 (E), whereas a lesser number of positives were apparent in non-Tg (B) or *gad* mice (C). Most of these positive cells appeared to be primary spermatocytes. Magnification: (A) ×100; (B–E) ×400. Scale bar in (A) 200 μm; (E) 50 μm.

UCH-L1 Relates to the Expression of PCNA

PCNA expression is associated with cell proliferation and DNA synthesis during S phase of the cell cycle and DNA repair in non-dividing cells (Kelman, 1997; Toschi and Bravo, 1988). Unlike UCH-L1, which is abundant in brain, PCNA is not detectable in the central nervous system (Saigoh et al., 1999; Williams et al., 2002). In the testis, PCNA is expressed in germ cells and Sertoli cells, and the nuclear localization of PCNA overlaps with that of UCH-L1 in monkey testis (Tokunaga et al., 1999). Our recent study showed that mice lacking UCH-L1 have significantly decreased numbers of PCNA-positive cells in seminiferous tubules (Kwon et al., 2003). These results led us to hypothesize that UCH-L1 may be closely associated with spermatogonial proliferation activity, possibly to maintain the primordial nature of these cells. We thus immunostained testes for PCNA

and UCH-L1. In non-Tg and *gad* testes, PCNA-positive staining was confined to spermatogonia and primary spermatocytes and was not evident in Sertoli cells (Fig. 4A,D,B,E) Similarly, the percentage of PCNA-positive spermatogonia and spermatocytes in the seminiferous tubules of *gad* mice was significantly lower than that of non-Tg mice (Fig. 4A,D,B,E) as we previously observed (Kwon et al., 2003). In contrast, Tg mouse testes showed greater PCNA staining in these cells; surprisingly however, staining was observed in nearly all arrested primary spermatocytes but not in spermatogonia (Fig. 4F). These findings suggest that UCH-L1 plays a specific role in mitotic proliferation. To further clarify the effect of UCH-L1 on PCNA levels, FLAG-tagged *Uchl1* was transfected into GC-1, a germ cell line derived from type B spermatogonia (Hofmann et al., 1992). UCH-L1 (anti-FLAG, Fig. 4G,I, green) and PCNA (Fig. 4H,I, red) were then visualized using immunofluorescence microscopy. Cells transfected with *Uchl1* showed lower PCNA immunoreactivity compared with mock-transfected cells (Fig. 4G), consistent with the assertion that PCNA is downregulated by UCH-L1 in vivo. However, no change of PCNA level was observed in *Uchl3* transfected cells (data not shown),

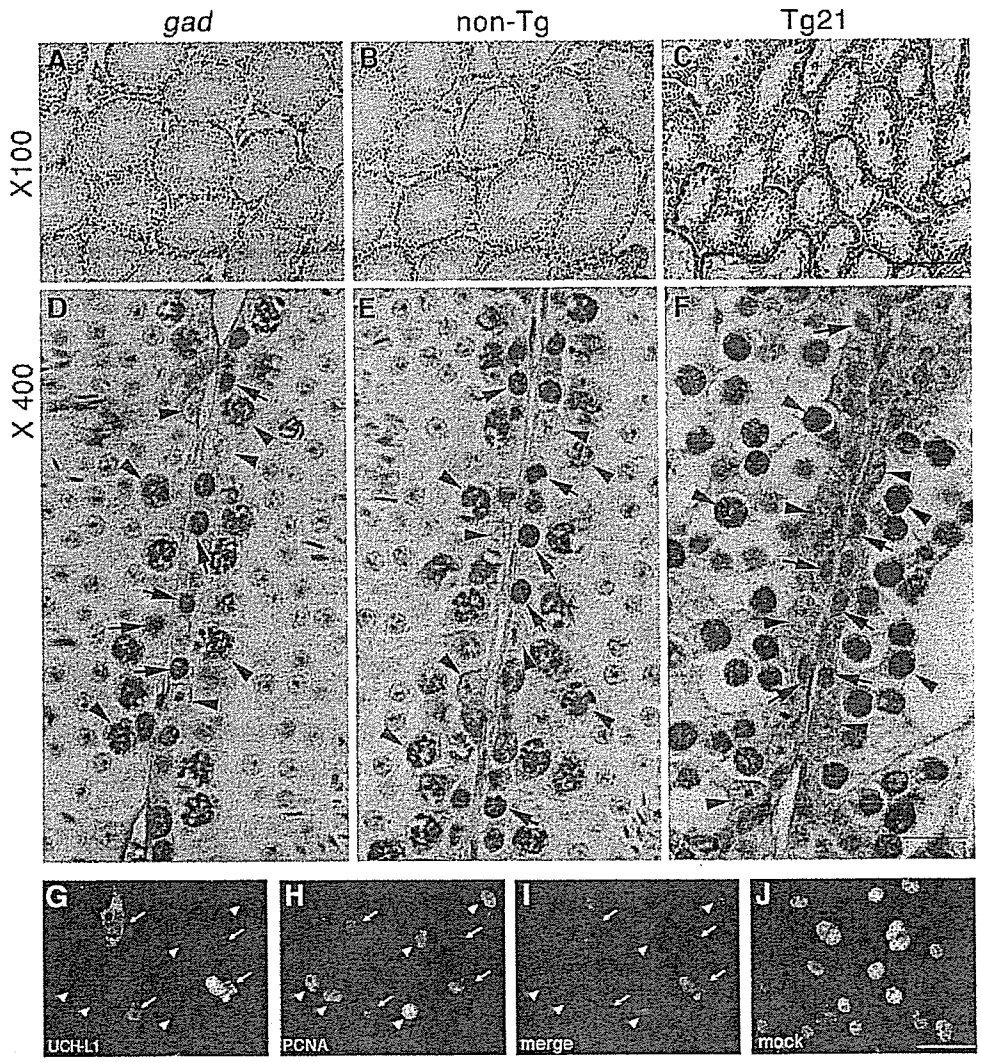

Fig. 4. PCNA immunostaining in the testes of a *gad* mouse (**A, D**), a non-Tg mouse (**B, E**), a Tg mouse (**C, F**; Tg21), and in the transient transfection assay with UCH-L1 using GC-1 cells (**G–J**). In *gad* and non-Tg testes, positive immunostaining was confined to spermatogonia (D, E; black arrows) and primary spermatocytes (D, E; red arrowheads), and staining was not seen in Sertoli cells (D, E; black arrowheads). In contrast, cell staining was more intense in the testis of Tg mice; however, this intensity was observed in almost all arrested primary spermatocytes (F; red arrowheads) but not in spermatogonia (F; black arrows). The staining of non-Tg and *gad* mice was essentially identical. However, nearly all the primary spermatocytes from Tg mice had relatively strong reactivity compared with spermatogonia that had very faint PCNA reactivity (black arrows). Plasmid pCIneo-*Uchl1* (G–I) or vector alone (J, mock) was transfected into GC-1 cells and expressed. Antibodies against FLAG (Sigma, monoclonal) and PCNA (BD Transduction Laboratory, polyclonal) were used to detect exogenously expressed UCH-L1 (G, I, green) and endogenous PCNA (H, J, I, red), respectively. Cells expressing a high level of UCH-L1 (G, white arrows) had a relative low level of PCNA (H, white arrows), whereas cells expressing a low level of UCH-L1 (H, white arrowheads) had high PCNA levels (H, white arrowheads). Magnification: (A–C) ×100; (D–J) ×400. Scale bar: **Upper panels** (see **panel C**), 200 μm; **middle panels** (see **panel F**), 50 μm; **lower panels** (see **panel J**), 50 μm.

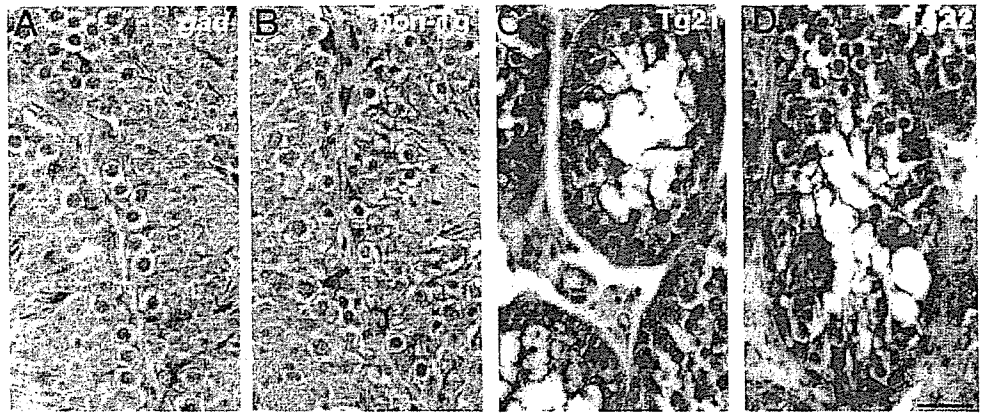

Fig. 5. Vimentin immunostaining in the testes of a *gad* mouse (**A**), a non-Tg mouse (**B**), and Tg mice (**C**, Tg21; **D**, Tg22). No difference was observed in the pattern and density of vimentin staining in Sertoli cells between *gad* (A) and non-Tg testes (B). In contrast, Sertoli cell staining was more intense in the Tg mice (C, D). Magnification: ×400. Scale bar, 200 μm.

suggesting the specificity of UCH-L1 effect on PCNA levels.

Sertoli Cells Exhibit High-Level Vimentin Expression in Tg Mice

We examined the immunoreactivity to vimentin, which is a marker of Sertoli cells (Oke and Suarez-Quian, 1993; Mori et al., 1997). Vimentin immunostaining was observed in Sertoli cells, and there is no difference between *gad* and non-Tg mice (Fig. 5A,B). In contrast, very strong expression of vimentin was observed in almost all Sertoli cells throughout the cytoplasm in Tg mice (Fig. 5C,D).

Bcl-2 Downregulation and Caspase-3 Upregulation in Tg Mice

The two key proteins, Bcl-2 and caspases-3 that involved in testicular germ cell apoptosis are especially altered during spermatogenesis or stress-induced germ cell apoptosis in *gad*mice (Harada et al., 2004; Kwon et al., 2004b, 2005). We thus examined the expression of these proteins in Tg and non-Tg testes to determine whether they are actually involved in countering increased apoptosis. Bcl-2 expression was downregulated in the testes of Tg mice compared with non-Tg mice (Fig. 6). In contrast to non-Tg mice, Tg mice had an elevated level of the activated caspase-3 subunit, p17 (Fig. 6), controversial to that observed in the retina of *gad* mice after ischemic injury (Harada et al., 2004). These results are consistent with the profound difference in UCH-L1 expression in these two mouse lines.

Upregulations of both Mono- and Poly-Ubiquitin in Tg Mice

Our recent studies suggested novel functions for UCH-L1, namely that it effectively upregulates ubiquitin levels at the post-transcriptional level (Osaka et al., 2003) and that ubiquitin induction plays a critical role in regulating cell death during cryptorchid injury–mediated germ cell apoptosis (Kwon et al., 2004b). Moreover, the testes of mice expressing K48R mutant ubiquitin are protected from cryptorchid injury (Rasoulpour et al., 2003). Given this information, we examined ubiquitin levels in *Uchl1* Tg mice. As expected, ubiquitin expression was strong in testicular cells of Tg mice (Fig. 7C,D), particularly in the arrested spermatocytes, but its expression was low in *gad* mice (Fig. 7B) compared with non-Tg mice (Fig. 7A). These data provide additional evidence that ubiquitin expression is induced upon UCH-L1 overexpression. To determine whether the increased ubiquitin staining represented monoubiquitin or polyubiquitin, we next examined the levels of both ubiquitin forms via immunoblotting (Fig. 7E). As expected, mono- and poly-ubiquitin levels in Tg mice were substantially higher than in non-Tg mice. A *gad* mouse control had relatively low levels

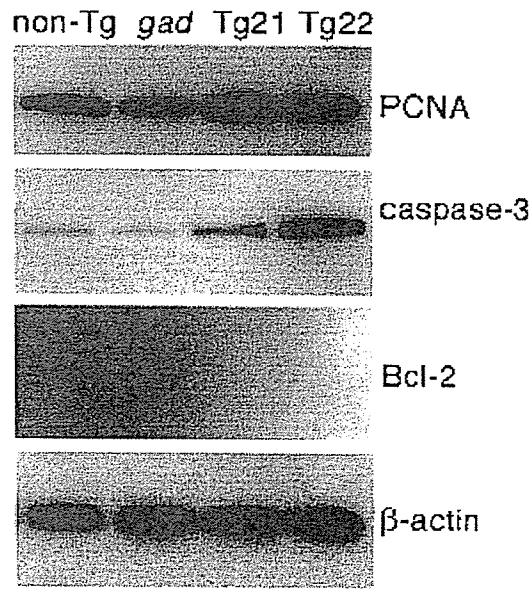

Fig. 6. Western blot analysis of Tg mouse testicular lysates. Consistent with the immunohistochemistry results, PCNA and caspase-3 substantially accumulated in Tg mice. However, the expression of antiapoptotic Bcl-2 decreased compared with non-Tg or *gad* mice.

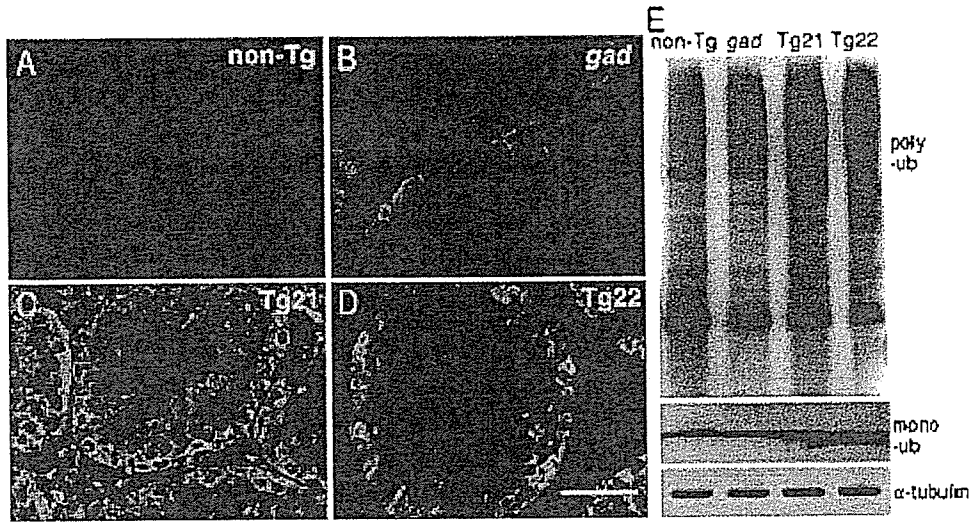

Fig. 7. The levels of mono- and poly-ubiquitin in the testes of non-Tg and Tg males. Double immunostaining for UCH-L1 and ubiquitin in the testis (**A**, non-Tg; **B**, *gad*; **C**, Tg21; **D**, Tg22). All strongly UCH-L1-positive cells (green) were also strongly positive for ubiquitin (red) in the two male Tg mice. Scale bar, 50 μm. **E**. An immunoblot showing that both mono- and poly-ubiquitin expression were significantly increased in the two Tg mice compared with non-Tg and *gad* mice (ub, ubiquitin).

of both mono- and poly-ubiquitin (Fig. 7E). These findings are consistent with previous studies and support the hypothesis that UCH-L1-mediated spermatocyte apoptosis involves the induction of ubiquitin expression.

DISCUSSION

Apoptosis in testicular germ cells is regulated by a complicated signal transduction pathway; however, the molecular mechanisms regulating this process are uncertain. We recently showed that *gad* mice, lacking UCH-L1 function, are resistant to apoptotic stress (Harada et al., 2004; Kwon et al., 2004b). These observations conclusively indicate that UCH-L1 plays a role in germ cell death during experimental stress-induced apoptosis. We thus hypothesized that germ cell apoptosis is directly induced by excess UCH-L1. To test this hypothesis, we utilized three mouse lines, wild-type (non-Tg), *gad* and *Uchl1* Tgs, which differ with respect to UCH-L1 expression. In Tg mice, germ cell apoptosis was barely detectable in spermatogonia or Sertoli cells, both of which strongly expressed UCH-L1. Apoptosis was observed mainly in primary spermatocytes, which had weak or negative UCH-L1 expression although they are derived from spermatogonia. These data suggest that excess UCH-L1 in fact does not directly induce apoptosis in spermatogonia or somatic Sertoli cells. These data further provoke the question of why apoptosis occurs during spermatocyte meiosis.

In our *Uchl1* Tg mice, there was no evidence of spermatogonia or Sertoli cell apoptosis despite the fact that these cells had stronger UCH-L1 expression compared with non-Tg mice. Accordingly, it could be concluded that overexpression of UCH-L1 in spermatogonia does not directly induce apoptosis in these cells (nor in Sertoli cells). Because spermatocytes are genetically distinct from the original mother cell (spermatogonia), we speculate that the Tg mice are highly susceptible to spermatocyte apoptosis in vivo, with the inference that spermatocytes seem to be particularly sensitive to UCH-L1 overexpression in spermatogonia even though spermatocytes themselves express a much lower level of UCH-L1. In contrast, *gad* mice are resistant to cryptorchid-induced germ cell apoptosis, and many germ cells undergo apoptosis in older animals although their testes develop nearly normally and produce mature sperm (Kwon et al., 2004b). These data suggest that the lack of UCH-L1 causes mice to have lower sensitivity to stress compared with wild-type males, although UCH-L1 is probably not essential for spermatogenesis under normal conditions. On one hand, UCH-L1 seems to be necessary for the stabilization of germ cells to protect against aging-associated apoptosis; however, the stabilization of germ cells appears to be limited by the concentration of UCH-L1, and consequently they may be damaged during spermatocyte meiosis when UCH-L1 is overexpressed. Despite the fact that excess UCH-L1 does not induce spermatogonial apoptosis, abnormalities in intracellular regulatory factors may potentially influence mitosis directly (i.e., as the cell divides into two daughter cells—spermatocytes). Some of these factors may accumulate or be reduced in the presence of excess UCH-L1, thereby causing disruptions such as arrested meiosis or the onset of apoptosis in spermatocytes rather than spermatogonia (Fig. 8).

Many of the factors involved in cellular apoptosis, including the Bcl-2 family and caspases, are targets for ubiquitynation. Previously, we have shown that Bcl-2 is upregulated (Kwon et al., 2004b) and caspases-3 is downregulated (Kwon et al., 2005) in *gad* mice. The decreased level of Bcl-2 and increased level of caspases-3

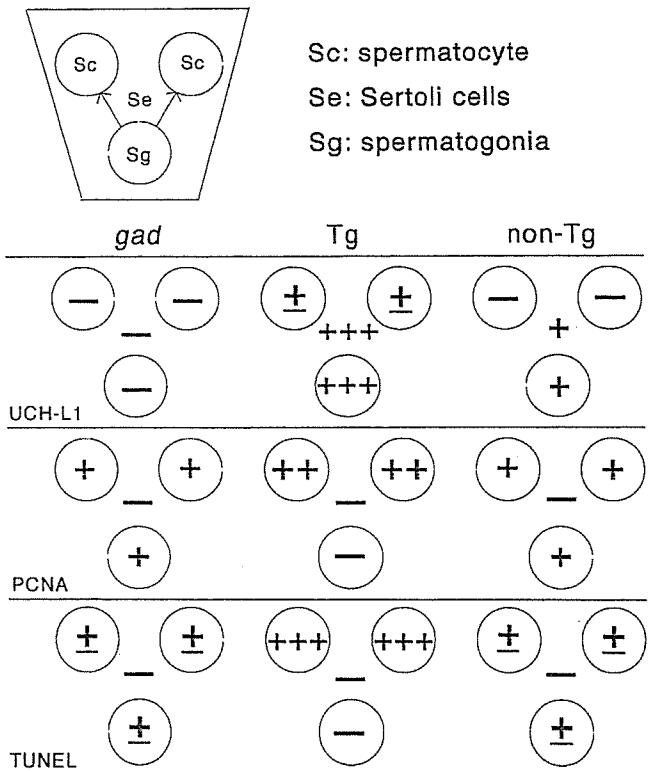

Fig. 8. TUNEL activity, and UCH-L1 and PCNA immunoreactivities in seminiferous tubules of non-Tg, *gad* and Tg mice. TUNEL activity or immunoreactivity: +++, strong; ++, moderate; + to ±, low to weak; −, not detectable.

observed in Tg mice in this study suggest that UCH-L1 can regulates the apoptosis during spermatogenesis by influencing the balance between apoptotic and anti-apoptotic proteins.

PCNA is ubiquitylated at lysine 48 (K48) and degraded by the ubiquitin-proteasome system (Yamamoto et al., 2004). In addition, PCNA is also monoubiquitylated at K164, thereby priming K63-linked polyubiquitin chains, which unlike K48-linked chains, do not promote proteasomal degradation (Hoege et al., 2002). In our present study, excess UCH-L1 relocalized PCNA from spermatogonia to spermatocytes and Sertoli cells in vivo and reduced PCNA expression to a low level in vitro. Based on these data, we hypothesize that UCH-L1, at least in part, may influence germ cell meiosis by affecting PCNA ubiquitynation, thereby disrupting its localization. In fact, PCNA significantly accumulated in primary spermatocytes of Tg mice (Fig. 4F). Since we did not obtain data regarding PCNA ubiquitylation in Tg mice, it is not clear whether the accumulated PCNA we observed was monoubiquitylated or polyubiquitylated. In any case, the accumulation of PCNA in primary spermatocytes may alter, damage or interrupt physical functions during meiosis (Fig. 8).

Germ cells and Sertoli cells are the only cell types expressed inside seminiferous tubules (McLaren, 1998). Germ cells constitute the male meiotic contribution to the reproductive cycle, whereas Sertoli cells support the growth and differentiation of germ cells. Direct interaction between germ cells and Sertoli cells may constitute an important part of the regulation of spermatogenesis (Russell et al., 1993). Indeed, mice exposed to Sertoli cell toxicants exhibit increased germ cell apoptosis (Lee et al., 1999). Therefore, Sertoli cells play a special role in nurturing and controlling spermatogenesis. Until postnatal day 16, UCH-L1 localizes only to spermatogonia, whereas after day 30 it also appears in Sertoli cells (Kon et al., 1999). Therefore, although UCH-L1 is highly expressed in both spermatogonia and somatic Sertoli cells, its function may be cell type-dependent. Under normal conditions UCH-L1 is a marker for activated Sertoli cells, in which it plays an important role in the degradation of abnormal proteins via the ubiquitin-proteasome system (Kon et al., 1999). Thus, we suspect that germ cell apoptosis in Tg mice might be related to the abnormal physical conditions in these cells. Our present work demonstrates that Tg mouse Sertoli cells are intensely immunoreactivity for UCH-L1, as expected. Furthermore, with vimentin, which is a marker present only in Sertoli cells (Oke and Suarez-Quian, 1993; Mori et al., 1997), we showed in this study that Tg mice had more vimentin immunoreactivity than non-Tg or *gad* mice (Fig. 5). Thus, forced expression of UCH-L1 in Sertoli cells perhaps may lead to gain of UCH function, thereby interrupting Sertoli cell-germ cell interactions that in turn promote germ cell apoptosis (Fig. 8).

In conclusion, we have demonstrated that UCH-L1 is an important spermatogenic factor related to PCNA and ubiquitin function. We used Tg mice overexpressing UCH-L1 to identify a new role for this protein. Overexpression of the *Uchl1* transgene inhibited spermatogenesis and induced germ cell death via an apoptotic mechanism, leading to male sterility. To our knowledge, the present data constitute the first description of a proapoptotic role for UCH-L1 in *Uchl1* Tg mice, as clearly revealed by the morphological and TUNEL results. Although UCH-L1 is constitutively expressed during spermatogenesis, and spermatogenic cell apoptosis is a normal aspect of mammalian spermatogenesis (Allan et al., 1992; Furuchi et al., 1996), the frequent cell death found in our *Uchl1* Tg mice could reflect an exaggeration of naturally occurring apoptosis. However, at present we do not understand whether the *Uchl1* transgene acts solely by inducing apoptosis or by interfering with differentiation so as to cause germ cell loss. This issue must be addressed to more fully define the role of UCH-L1 in the regulation and fate of spermatogonia during spermatogenesis.

ACKNOWLEDGMENTS

We thank H. Kikuchi for assistance in preparing the sections and M. Shikama for the care and breeding of animals.

REFERENCES

Allan DJ, Harmon BV, Roberts SA. 1992. Spermatogonial apoptosis has three morphologically recognizable phases and shows no circadian

rhythm during normal spermatogenesis in the rat. Cell Prolif 25: 241–250.

Aoki S, Su Q, Li H, Nishikawa K, Ayukawa K, Hara Y, Namikawa K, Kiryu-Seo S, Kiyama H, Wada K. 2002. Identification of an axotomy-induced glycosylated protein, AIGP1, possibly involved in cell death triggered by endoplasmic reticulum-Golgi stress. J Neurosci 22: 10751–10760.

Baarends WM, van der Laan R, Grootegoed JA. 2000. Specific aspects of the ubiquitin system in spermatogenesis. J Endocrinol Invest 23: 597–604.

Furuchi T, Masuko K, Nishimune Y, Obinata M, Matsui Y. 1996. Inhibition of testicular germ cell apoptosis and differentiation in mice misexpressing Bcl-2 in spermatogonia. Development 122: 1703–1709.

Harada T, Harada C, Wang YL, Osaka H, Amanai K, Tanaka K, Takizawa S, Setsuie R, Sakurai M, Sato Y, Noda M, Wada K. 2004. Role of ubiquitin carboxy terminal hydrolase-L1 in neural cell apoptosis induced by ischemic retinal injury in vivo. Am J Pathol 164:59–64.

Hoege C, Pfander B, Moldovan GL, Pyrowolakis G, Jentsch S. 2002. RAD6-dependent DNA repair is linked to modification of PCNA by ubiquitin and SUMO. Nature 419:135–141.

Hofmann MC, Narisawa S, Hess RA, Millan JL. 1992. Immortalization of germ cells and somatic testicular cells using the SV40 large T antigen. Exp Cell Res 201:417–435.

Imâi T, Kawai Y, Tadokoro Y, Yamamoto M, Nishimune Y, Yomogida K. 2004. In vivo and in vitro constant expression of GATA-4 in mouse postnatal Sertoli cells. Mol Cell Endocrinol 214:107–115.

Kelman Z. 1997. PCNA: Structure, functions, and interactions. Oncogene 14:629–640.

Kon Y, Endoh D, Iwanaga T. 1999. Expression of protein gene product 9.5, a neuronal ubiquitin C-terminal hydrolase, and its developing change in sertoli cells of mouse testis. Mol Reprod Dev 54:333–341.

Kroll KL, Amaya E. 1996. Transgenic *Xenopus* embryos from sperm nuclear transplantations reveal FGF signaling requirements during gastrulation. Development 122:3173–3183.

Kurihara LJ, Kikuchi T, Wada K, Tilghman SM. 2001. Loss of Uch-L1 and Uch-L3 leads to neurodegeneration, posterior paralysis, and dysphagia. Hum Mol Genet 10:1963–1970.

Kwon J, Kikuchi T, Setsuie R, Ishii Y, Kyuwa S, Yoshikawa Y. 2003. Characterization of the testis in congenitally ubiquitin carboxy-terminal hydrolase-1 (Uch-L1) defective (gad) mice. Exp Anim 52: 1–9.

Kwon J, Wang YL, Setsuie R, Sekiguchi S, Sakurai M, Sato Y, Lee WW, Ishii Y, Kyuwa S, Noda M, Wada K, Yoshikawa Y. 2004a. Developmental regulation of ubiquitin C-terminal hydrolase isozyme expression during spermatogenesis in mice. Biol Reprod 71: 515–521.

Kwon J, Wang YL, Setsuie R, Sekiguchi S, Sato Y, Sakurai M, Noda M, Aoki S, Yoshikawa Y, Wada K. 2004b. Two closely related ubiquitin C-terminal hydrolase isozymes function as reciprocal modulators of germ cell apoptosis in cryptorchid testis. Am J Pathol 165:1367–1374.

Kwon J, Mochida K, Wang YL, Sekiguchi S, Sankai T, Aoki S, Ogura A, Yoshikawa Y, Wada K. 2005. Ubiquitin C-terminal hydrolase L-1 is essential for the early apoptotic wave of germinal cells and for sperm quality control during spermatogenesis. Biol Reprod 73:29–35.

Lee J, Richburg JH, Shipp EB, Meistrich ML, Boekelheide K. 1999. The Fas system: A regulator of testicular germ cell apoptosis, is differentially up-regulated in Sertoli cell versus germ cell injury of the testis. Endocrinology 140:852–858.

Matzuk MM, Lamb DJ. 2002. Genetic dissection of mammalian fertility pathways. Nat Cell Biol 4:s41–s49.

McLaren A. 1998. Gonad development: Assembling the mammalian testis. Curr Biol 8:R175–R177.

Mizushima S, Nagata S. 1990. pEF-BOS: A powerful mammalian expression vector. Nucleic Acids Res 18:5322.

Mori C, Nakamura N, Dix DJ, Fujioka M, Nakagawa S, Shiota K, Eddy EM. 1997. Morphological analysis of germ cell apoptosis during postnatal testis development in normal and Hsp 70-2 knockout mice. Dev Dyn 208:125–136.

Oke BO, Suarez-Quian CA. 1993. Localization of secretory, membrane-associated, and cytoskeletal proteins in rat testis using an improved immunocytochemical protocol that employs polyester wax. Biol Reprod 48:621–631.

Osaka H, Wang YL, Takada K, Takizawa S, Setsuie R, Li H, Sato Y, Nishikawa K, Sun YJ, Sakurai M, Harada T, Hara Y, Kimura I, Chiba S, Namikawa K, Kiyama H, Noda M, Aoki S, Wada K. 2003. Ubiquitin carboxy-terminal hydrolase L1 binds to and stabilizes monoubiquitin in neuron. Hum Mol Genet 12:1945–1958.

Osawa Y, Wang YL, Osaka H, Aoki S, Wada K. 2001. Cloning, expression, and mapping of a mouse gene, *Uchl4*, highly homologous to human and mouse Uchl3. Biochem Biophys Res Commun 283: 627–633.

Rasoulpour RJ, Schoenfeld HA, Gray DA, Boekelheide K. 2003. Expression of a K48R mutant ubiquitin protects mouse testis from cryptorchid injury and aging. Am J Pathol 163:2595–2603.

Russell LD, Corbin TJ, Borg KE, De Franca LR, Grasso P, Bartke A. 1993. Recombinant human follicle-stimulating hormone is capable of exerting a biological effect in the adult hypophysectomized rat by reducing the numbers of degenerating germ cells. Endocrinology 133:2062–2070.

Saigoh K, Wang YL, Suh JG, Yamanishi T, Sakai Y, Kiyosawa H, Harada T, Ichihara N, Wakana S, Kikuchi T, Wada K. 1999. Intragenic deletion in the gene encoding ubiquitin carboxy-terminal hydrolase in gad mice. Nat Genet 23:47–51.

Sutovsky P. 2003. Ubiquitin-dependent proteolysis in mammalian spermatogenesis, fertilization, and sperm quality control: Killing three birds with one stone. Microsc Res Tech 61:88–102.

Tokunaga Y, Imai S, Torii R, Maeda T. 1999. Cytoplasmic liberation of protein gene product 9.5 during the seasonal regulation of spermatogenesis in the monkey (*Macaca fuscata*). Endocrinology 140:1875–1883.

Toschi L, Bravo R. 1988. Changes in cyclin/proliferating cell nuclear antigen distribution during DNA repair synthesis. J Cell Biol 107: 1623–1628.

Wilkinson KD. 2000. Ubiquitination and deubiquitination: Targeting of proteins for degradation by the proteasome. Semin Cell Dev Biol 11:141–148.

Williams K, Schwartz A, Corey S, Orandle M, Kennedy W, Thompson B, Alvarez X, Brown C, Gartner S, Lackner A. 2002. Proliferating cellular nuclear antigen expression as a marker of perivascular macrophages in simian immunodeficiency virus encephalitis. Am J Pathol 161:575–585.

Wing SS. 2003. Deubiquitinating enzymes—the importance of driving in reverse along the ubiquitin-proteasome pathway. Int J Biochem Cell Biol 35:590–605.

Yamamoto T, Kimura S, Mori Y, Oka M, Ishibashi T, Yanagawa Y, Nara T, Nakagawa H, Hashimoto J, Sakaguchi K. 2004. Degradation of proliferating cell nuclear antigen by 26S proteasome in rice (*Oryza sativa* L.). Planta 218:640–646.

Yamazaki K, Wakasugi N, Tomita T, Kikuchi T, Mukoyama M, Ando K. 1988. Gracile axonal dystrophy (GAD): A new neurological mutant in the mouse. Proc Soc Exp Biol Med 187:209–215.

Yuan L, Liu JG, Zhao J, Brundell E, Daneholt B, Hoog C. 2000. The murine *SCP3* gene is required for synaptonemal complex assembly, chromosome synapsis, and male fertility. Mol Cell 5:73–83.

PEPTIDES 27 (2006) 3176–3182

available at www.sciencedirect.com

ScienceDirect

journal homepage: www.elsevier.com/locate/peptides

Effect of β-lactotensin on acute stress and fear memory

Rena Yamauchi [a,c,d], Etsuko Wada [a,d,*], Daisuke Yamada [a,d], Masaaki Yoshikawa [b,d], Keiji Wada [a,d]

[a] Department of Degenerative Neurological Diseases, National Institute of Neuroscience, National Center of Neurology and Psychiatry, Kodaira, Tokyo 187-8502, Japan
[b] Division of Food Science and Biotechnology, Graduate School of Agriculture, Kyoto University, Uji, Kyoto 611-0011, Japan
[c] Japan Society for Promotion of Science, Chiyoda-ku, Tokyo 104-8471, Japan
[d] CREST, Japan Science and Technology Agency, Kawaguchi, Saitama 322-0012, Japan

ARTICLE INFO

Article history:
Received 5 May 2006
Received in revised form
11 August 2006
Accepted 11 August 2006
Published on line 26 September 2006

Keywords:
Neurotensin
β-Lactotensin
Anti-stress
Hole-board test
Fear memory

ABSTRACT

β-Lactotensin (β-LT) is a bioactive peptide derived from bovine milk β-lactoglobulin and is a natural ligand for neurotensin receptors. We examined the effect of β-LT on restraint stress and fear memory in mice. Mice subjected to acute restraint stress exhibited a decreased number of head-dips and increased head-dip latency compared to non-stressed controls in the hole-board test, reflecting increased stress-induced behaviors. However, prior administration of β-LT improved the behaviors caused by stress. The anti-stress effect of β-LT was blocked by levocabastine, a neurotensin receptor subtype 2 (NTR2) antagonist. In the fear-conditioning test, the duration of freezing responses by cued fear conditioning was significantly reduced in mice administered β-LT compared with control mice. These results suggest that β-LT has an anti-stress effect and promotes the extinction of fear memory, which may be mediated by NTR2.

© 2006 Elsevier Inc. All rights reserved.

1. Introduction

Many bioactive peptides are derived from food proteins (e.g., β-casomorphin, ovokinin and gluten exorphin) [7,8,11]. These peptides elicit various biological effects, such as antinociception, hypotension and enhancement of learning and memory [4,19,21,27]. We previously isolated a 4-residue bioactive peptide β-lactotensin (β-LT; His-Ile-Arg-Leu) from a chymotrypsin digest of β-lactoglobulin [33]. We showed that β-LT is a natural ligand for neurotensin receptors (NTRs) [33]. There are three subtypes of NTRs. NTR subtype 1 (NTR1) [29] and subtype 2 (NTR2) [14] have high- and low-affinity neurotensin binding sites, respectively, and are G-protein-coupled receptors with seven-transmembrane domains. NTR subtype 3 (NTR3), however, is a receptor with single-transmembrane domain [15]. β-LT binds to both NTR1 and NTR2, and the binding affinity of β-LT to NTR2 was about 50-fold higher than to NTR1 [33]. While our in vivo studies of β-LT in mice showed that NTR2 peripherally mediates a hypocholesterolemic and antinociceptive effects [34,35], the effects of β-LT on higher brain function such as learning, memory, fear and anxiety have not been investigated. To date, there are some studies in rodents that have investigated the effect of neurotensin on behavior (e.g., food intake, locomotor activity and emotional behavior) [13,22,23]. Centrally administered neurotensin has been shown to stimulate the hypothalamic-pituitary-adrenal (HPA) axis in rat [18], suggesting that neurotensin can modulate stress response or other emotional status. In the central nervous system (CNS), NTR1

* Corresponding author at: Department of Degenerative Neurological Diseases, National Institute of Neuroscience, National Center of Neurology and Psychiatry, Ogawahigashi 4-1-1, Kodaira, Tokyo 187-8502, Japan. Tel.: +81 42 346 1715; fax: +81 42 346 1745.
E-mail address: wada_e@ncnp.go.jp (E. Wada).
0196-9781/$ – see front matter © 2006 Elsevier Inc. All rights reserved.
doi:10.1016/j.peptides.2006.08.009

mRNA expression has been observed in the thalamus, hypothalamus and the midbrain [2], whereas NTR2 mRNA is diffusely expressed throughout the brain [20]. NTR2 mRNA is expressed in the cortex and limbic region such as hippocampus, hypothalamus and amygdala [20]. These regions are important in the modulation of emotion and fear memory [5,10]. To examine the effect of β-LT on emotional behavior and fear memory, we performed the behavioral tests using β-LT. Among various kinds of emotional behavioral tests, we performed the hole-board test, because the hole-board test is one of methods commonly used for determining the anti-stress behavior. In addition, we performed the fear-conditioning test to examine the effect of β-LT on learning and memory, since the neuronal circuit for fear memory is well investigated. We also examined the effect of an NTR2 antagonist on mice pretreated with β-LT.

2. Materials and methods

2.1. Animals

Male C57BL/6J mice (8–9 weeks old) were used for all behavioral experiments. Mice were kept in a temperature and humidity-controlled room with a 12-h light–dark cycle (lights on at 08:00). Food and water were available ad libitum. All behavioral experiments were performed between 11:00 and 16:00 during the light cycle. All animal experiments were performed in strict accordance with the guidelines of the National Institutes of Neuroscience, National Center of Neurology and Psychiatry (Japan) and were approved by the Animal Investigation Committee of the Institute.

2.2. Reagents

β-LT (His-Ile-Arg-Leu; MW 537.7) was synthesized by American Peptide Company (Sunnyvale, CA) according to our order. β-LT was dissolved in saline and adjusted to pH 7.0 before administration to animals. Levocabastine hydrochloride was obtained from BIOMOL Research Laboratories Inc. (Plymouth Meeting, PA) and dissolved in saline with 5% dimethyl sulfoxide.

2.3. Hole-board test

The hole-board experiments were performed using a hole-board system (O'Hara & Co., Ltd., Japan) consisting of vinyl chloride board (50 cm × 50 cm) with equally placed four holes (3 cm diameter). The analysis of images was performed on a Macintosh computer using Image OFC 2.03x and Image OF 2.15x (O'Hara & Co., Ltd., Japan), a modified program based on NIH Image program. The program is a freeware developed by the U.S. National Institutes of Health and available on the internet at http://rsb.info.nih.gov/nih-image/. The experimental chamber was illuminated at 170 lx. The condition of restraint and the timing of drug injection were performed as described by Tsuji et al. [30]. Mice were either restrained in a 50 mL corning tube for 60 min (stressed group) or left in their home cage (non-stressed group). After release from restraint, β-LT (10 or 30 mg/kg) or saline (10 μL/g, control) was administered intraperitoneally. After 30 min, the hole-board test was performed and four parameters were measured for 5 min. The four parameters measured were: the number of head-dips, manually counted each time when mouse dipped its nose into the hole; the head-dipping latency which was the time elapsed before the first head-dip; total locomotor activity which was measured as the total moving distance of mouse measured in cm; the rate of visitation to the center area (referred to here as "% center") of the board, calculated as: [% center = staying duration in center area (s)/total experimental duration (300 s) × 100]. These parameters are indicators of the emotional status of mice [30]. Levocabastine (0.05 mg/kg) was given 10 min after the administration of β-LT in order to observe the effect of an antagonist on the anti-stress effect of β-LT. The doses of β-LT and levocabastine were as described previously [34].

2.4. Fear-conditioning test

Fear-conditioning experiments were performed using a computerized fear-conditioning system (O'Hara & Co., Ltd., Japan). On the conditioning day, each mouse was placed in the conditioning chamber (10 cm × 10 cm × 12 cm, clear plastic) equipped with an electrified 10 cm × 10 cm floor grid for 2 min before the onset of a tone (70 dB, 10 kHz) that lasted for 30 s. A foot shock (0.5 mA) was delivered through the floor grid during the last 2 s of the tone. The mice received the foot shock two times with a 1 min interval. β-LT was administered intraperitoneally after the conditioning. The doses of β-LT was followed the previous report [34]. On the second day, the freezing behavior was examined for 3 min in the same chamber without the tone or footshock (contextual fear conditioning). On the third day, mice were placed in a new chamber (10 cm × 10 cm × 12 cm, white plastic) under red light (cued fear conditioning). After habituation period of 2 min, the same tone (70 dB, 10 kHz) that has been used during conditioning was given for 3 min. The contextual and the cued test were performed 24 h and 48 h after the conditioning, respectively. The two tests were also performed with the same mice 1 week and 3 weeks after the conditioning. The freezing score (%) was presented as the ratio of time spent in a freezing state during the experiment. The freezing images were analyzed on a Macintosh computer using Image FZC 2.22 (O'Hara & Co., Ltd., Japan), a modified program based on NIH Image program. The program is a freeware developed by the U.S. National Institutes of Health and available on the internet at http://rsb.info.nih.gov/nih-image/.

2.5. Statistical analysis

The values are presented as the mean ± S.E.M. Statistical analyses were performed using the unpaired Student's t-test or ANOVA (followed by Bonferroni's multiple comparison test). p values < 0.05 were considered statistically significant in all statistical tests.

3. Results

3.1. Hole-board test

3.1.1. Effect of β-LT on head-dipping behavior

At first, we performed the hole-board test under non-stress condition to examine the effect of β-LT on mouse behavior.

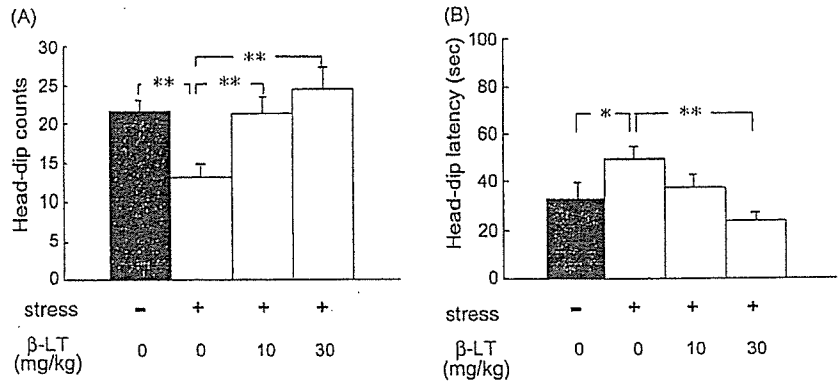

Fig. 1 – Effect of β-LT on the number of head-dips (A) and head-dipping latency (B) after stress/non-stress during the hole-board test. The hole-board test was performed 30 min after i.p. administration of β-LT. The values shown are mean ± S.E.M. ($n = 12$). $^{*}p < 0.05$ and $^{**}p < 0.01$ vs. control using the unpaired Student's t-test.

However, significant difference was not observed in any parameters between β-LT-treated mice and control mice (data not shown). Since there was no difference in the hole-board test without stress, we performed the hole-board test under restraint stress to examine the effect of β-LT on stressed mouse behavior. Sixty-minute restraint-induced stress decreased the number of head-dips compared with non-stressed control mice [non-stress: 21.67 ± 1.3; stress: 13.0 ± 1.78, $p < 0.01$] (Fig. 1A), in agreement with previous results [30]. Administration of β-LT significantly increased the number of head-dips after restraint stress compared with group treated with saline in a dose-dependent manner [β-LT 0 mg/kg: 13.0 ± 1.78; 10 mg/kg: 21.27 ± 2.09, $p < 0.01$; 30 mg/kg: 24.50 ± 2.57, $p < 0.01$]. The latency to the first head-dip was significantly extended in mice given restraint stress [non-stress: 32.63 ± 6.38 s; stress: 49.49 ± 5.15 s, $p < 0.05$] (Fig. 1B). Pretreatment with β-LT also improved the latency to the non-stressed control level in a dose-dependent manner [β-LT 0 mg/kg: 49.49 ± 5.15 s; 10 mg/kg: 37.33 ± 4.70 s; 30 mg/kg: 24.47 ± 2.76 s, $p < 0.01$].

3.2. *Effect of β-LT on spontaneous activity in the hole-board test*

To determine the spontaneous activity of mice that were pretreated with β-LT, total movement was examined using the hole-board test. In addition, the amount of time the mice spent in the defined center area (% center) was measured. Total locomotor activity and % center did not differ between the non-stressed and stressed control groups, and pretreatment with β-LT also did not affect these two behaviors (Fig. 2A and B). These results suggest that β-LT or restraint-induced stress does not affect spontaneous activity as measured by the hole-board test.

3.3. *Effect of an NTR2 antagonist on head-dipping behavior*

In our previous studies, we demonstrated that β-LT is a natural ligand for NTR2 and that some of the physiological effects of β-LT are mediated by NTR2 [34,35]. Thus, we investigated the effect of the NTR2 antagonist, levocabastine,

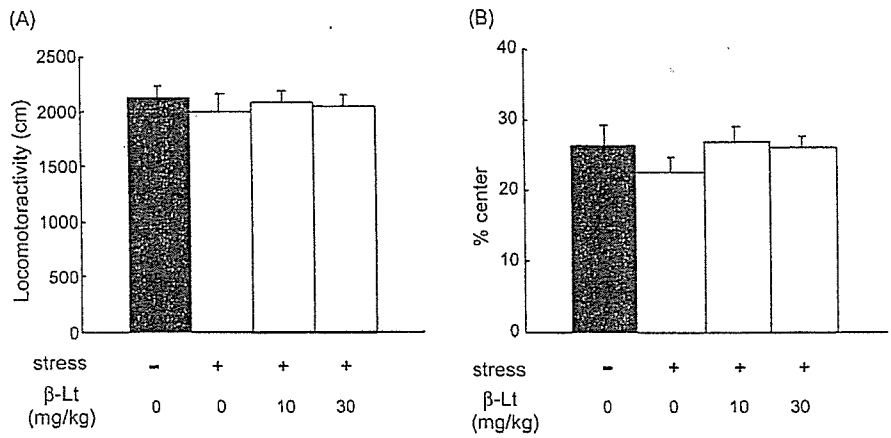

Fig. 2 – Effect of β-LT on total locomotor activity (A) and the rate of visitation to the center area (% center) (B) after stress/non-stress during the hole-board test. The hole-board test was performed 30 min after i.p. administration of β-LT. The values shown are mean ± S.E.M. ($n = 12$).

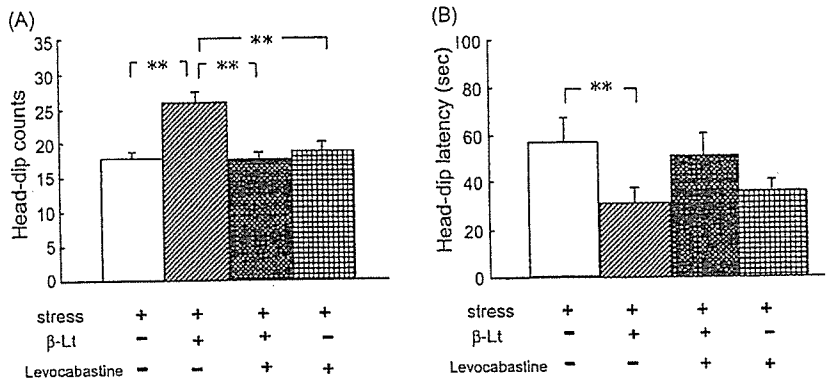

Fig. 3 – Effect of the NTR2 antagonist levocabastine on the number of head-dips (A) and head-dipping latency (B) after stress following the administration of β-LT during the hole-board test. β-LT was administered i.p. at a dose of 30 mg/kg. Levocabastine was given intraperitoneally at a dose of 0.05 mg/kg 10 min after β-LT administration. The values shown are mean ± S.E.M. ($n = 8$). $^{**}p < 0.01$ vs. control using ANOVA, followed by Bonferroni's multiple comparison test.

on mice pretreated with β-LT. In mice that received β-LT, levocabastine blocked the anxiolytic effect of β-LT and the number of head-dips decreased [levocabastine (−): 25.78 ± 1.59; levocabastine (+): 17.67 ± 1.01, $p < 0.01$] (Fig. 3A). Levocabastine tended to block the effect of β-LT in the head-dipping latency [levocabastine (−): 30.55 ± 6.04 s; levocabastine (+): 51.03 ± 9.24 s, $p = 0.06$] (Fig. 3B). Levocabastine itself did not affect these head-dipping behaviors. These results suggest that the anti-stress effect of β-LT on mouse behavior can be blocked by an NTR2 antagonist.

3.4. *Effect of β-LT on fear-conditioning test*

Prior to the experiments with β-LT administered mice, we tested with naive C57BL/6J mice to ascertain the validity of the fear-conditioning system. In the conditioning, mice habituated in the grid chamber (freezing: <1%). After two electrical shocks with tone, mice showed freezing response (27.9 ± 8.7%). In the contextual test at 24 h after conditioning, mice froze in the conditioned chamber (30.8 ± 10.9%). In the cued test, mice were freely moving in the novel chamber before the tone (<1%). After the tone stimulus, they froze in the chamber (26.3 ± 7.5%).

Thus, the validity of the fear-conditioning test was confirmed, and we performed next the fear-conditioning test to investigate the effect of β-LT on fear memory. There was no difference in freezing behavior among the three groups during the conditioning (data not shown). Immediately after the conditioning, β-LT was administered intraperitoneally. In order to give the same conditioning circumstance, β-LT was administered at this point. Contextual tests conducted at 24 h, 1 week and 3 weeks after the conditioning showed that contextual fear memory was not affected by β-LT treatment (Fig. 4A). On the other hand, cued test conducted 1 week after

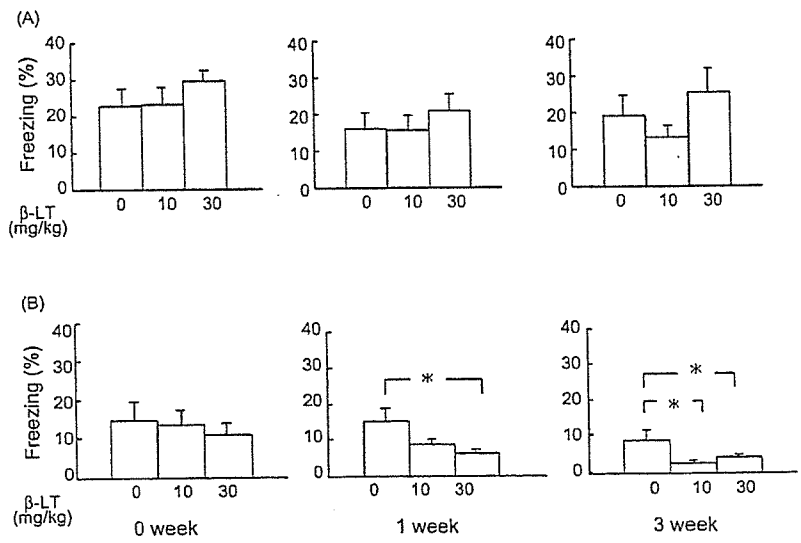

Fig. 4 – Effect of β-LT in the fear-conditioning test. (A) Effect of β-LT in the contextual test; (B) effect of β-LT in the cued test. Immediately after the conditioning, β-LT was administered intraperitoneally. The rate of freezing (%) was calculated to indicate fear memory. The values shown are mean ± S.E.M. ($n = 10$). $^{*}p < 0.05$ vs. control using the unpaired Student's t-test.

the conditioning showed that β-LT significantly decreased cued-fear memory in a dose-dependent manner [control: 14.27 ± 2.91%; β-LT 30 mg/kg: 6.03 ± 0.41%, $p < 0.05$] (Fig. 4B). In addition, the difference in freezing behavior between control mice and β-LT-treated mice was still evident at 3 weeks after the conditioning.

4. Discussion

In our present study, pretreatment of restraint-stressed mice with β-LT increased the number of head-dips and shortened the latency to the first head-dip compared to the control levels in the hole-board test. As we observed, Tsuji et al. [30] showed a significant decrease in the number of head-dips and a significant increase in head-dipping latency in mice 1hr after acute restraint-induced stress. Since there was no difference in the hole-board test without stress, our results suggest that β-LT has anti-stress effect on stressed mouse. Physical or psychological stress is known to activate the HPA axis [12], suggesting that peripheral administration of β-LT may modulate the activation of the HPA axis. The anti-stress effect by β-LT was blocked by levocabastine, an NTR2 antagonist. The Ki values of levocabastine for NTR1 and NTR2 are >10,000 nM and 17 ± 2 nM, respectively [17]. Although, levocabastine is an antagonist not only for NTR2 but also for histamine H1 receptor [14,32], it was shown that histamine H1 receptor was not involved in the head-dipping behavior in the hole-board test [3]. These results suggest that the blockade of the effect of β-LT is due to the inhibition of NTR2.

Though the intracellular signaling of NTR2 is very important, the mechanisms of signaling properties are still controversial. For example, when the receptors are expressed in mammalian cells or in *Xenopus oocytes*, the receptor shows different characters that may be species-dependent [31]. In addition, neurotensin acts as an antagonist in human NTR2 expressing in CHO cells though it acts as an agonist endogenously. Since the NTR2 is Gq-coupled type receptor, the signaling pathway may be mediated by Gq-related IP3 as a second messenger. β-LT may be a useful tool to investigate the signaling pathways downstream of NTR2.

In the cued fear-conditioning test, freezing response was significantly reduced in β-LT-treated mice 1 week after conditioning. In order to examine whether the effect of β-LT is mediated by NTR2, we tested the effect of levocabastine on the fear extinction effect of β-LT in the fear-conditioning test. Levocabastine reversed the reduction of freezing induced by β-LT (data not shown). However, levocabastine itself also reduced the freezing response in our study. We could not confirm the NTR2 blockade by levocabastine in the fear-conditioning test, while levocabastine could block the effect of β-LT in the hole-board test, suggesting the involvement of NTR2. One of the reasons for this discrepancy is that the timing of drug adminstration is different between the hole-board test and the fear-conditioning test. In addition, though levocabastine or histamine H1 receptor has not been reported to affect the fear memory, our results suggest that H1 receptor may be involved in fear conditioning.

In this study, during the conditioning session conducted prior to the fear-conditioning test, all mice froze (data not shown). This indicates the fear memory was normally acquired. And the results obtained from the subsequent contextual as well as cued tests, conducted after 24 h and 48 h, show that the fear memory was consolidated. However, generally this consolidation is not stable, and fear memory become labile when the animal is exposed to the same circumstance again, or the conditioned stimulus such as sound is given [1]. It has been reported that once the fear memory becomes labile, it will either consolidate or extinct [1,26]. In our study, the freezing response began to decrease 1 week after the conditioning. Consequently, two possible causes are considered; namely, consolidation of the fear memory may not be completed, and/or extinction of the fear memory may be promoted. Since consolidation and extinction are known to occur simultaneously, β-LT tends to destabilize memory consolidation and promote fear memory extinction.

There are several possibilities on how β-LT can promote the fear extinction. It is known that the fear extinction requires time-dependent novel protein synthesis. Stiedl et al. [25] showed that a protein synthesis inhibitor cycloheximide injection at posttraining in the fear-conditioning test promoted memory extinction 24 h after the first test. Thus, posttraining injection of β-LT may modulate the protein synthesis, and affect on the memory extinction process. Furthermore, Sotres et al. have reported that the inhibitory signal from ventral medial prefrontal cortex is transmitted to the lateral amygdala and induces the reduction of freezing response in the fear memory extinction process [24]. Our findings suggest another possibility that β-LT may promote the extinction of cued-fear memory by modulating the signal from the medial prefrontal cortex to the lateral amygdala.

Peripheral administration of peptides derived from milk protein can modulate anxiety-related behavior and distress [16,27]. Miclo et al. reported that i.p. administration of α-casozepine, a tryptic peptide from bovine milk casein, improved anxiety in the elevated plus maze and defensive burying test [16]. They showed that the antianxiety effect of α-casozepine may be mediated by the $GABA_A$ receptor. In pigs, orally infused colostrums, from which lactoferrin, a milk-derived peptide, is produced by enzymatic digestion, can be transported via circulating blood into the cerebrospinal fluid where it binds to the Lf receptor in the choloid plexus (CP) [9,28]. Flood et al. reported that i.p. administration of mammalian bombesin-like peptide, gastrin-releasing peptide (GRP), enhanced memory [6]. Vagotomy inhibits the memory-enhancing effects of GRP, suggesting that this peptide affects by activating ascending vagal pathways [6]. To date, the distribution of functional NTR2 in the CP and peripheral vagal ganglion has not been reported. Further investigation is needed to learn more about the mechanism of how β-LT affects the CNS.

Our present study shows that β-LT, which is derived from β-lactoglobulin, has an anti-stress effect and promotes the extinction of fear memory in the CNS. Given that anti-anxiety or anti-stress drugs sometimes induce adverse side effects such as drowsiness, thirst, and addiction, the fact that β-LT is a natural product from milk protein suggests that β-LT may be a safe and useful substance to modulate emotional disorders.

Acknowledgements

We thank Dr. Zushida for his instruction with regard to the hole-board test, and Mr. Takagaki and Ms. Tamura for editing of the manuscript. This work was supported by research grants from the Ministry of Health, Labor and Welfare of Japan, the Ministry of Education, Culture, Sports, Science and Technology of Japan, and CREST, the Japan Science and Technology Agency.

REFERENCES

[1] Abel T, Lattal KM. Molecular mechanisms of memory acquisition, consolidation and retrieval. Curr Opin Neurobiol 2001;11:180–7.
[2] Alexander MJ, Leeman SE. Widespread expression in adult rat forebrain of mRNA encoding high-affinity neurotensin receptor. J Comp Neurol 1998;402:475–500.
[3] Alvarez EO, Banzan AM. Histamine in dorsal and ventral hippocampus II. Effects of H1 and H2 histamine antagonists on exploratory behavior in male rats. Physiol Behav 1986;37:39–45.
[4] Chang KJ, Cuatrecasas P, Wei ET, Chang JK. Analgesic activity of intracerebroventricular administration of morphiceptin and β-casomorphins: correlation with the morphin (μ) receptor binding affinity. Life Sci 1982;30:1547–51.
[5] Delaney AJ, Sah P. GABA receptors inhibited by benzodiazepins mediate fast inhibitory transmission in the central amygdala. J Neurosci 1999;19:9698–704.
[6] Flood JF, Morley JE. Effects of bombesin and gastrin-releasing peptide on memory processing. Brain Res 1988;460:314–22.
[7] Fujita H, Usui H, Kurahashi K, Yoshikawa M. Isolation and characterization of ovokinin, a bradykinin B1 agonist peptide derived from ovalbumin. Peptides 1995;16:785–90.
[8] Fukudome S, Yoshikawa M. Opioid peptides derived from wheat gluten: their isolation and characterization. FEBS Lett 1992;296:107–11.
[9] Harada E, Sugiyama A, Takeuchi T, Sitizyo K, Syuto B, Yajima T, et al. Characteristic transfer of colostral components into cerebrospinal fluid via serum in neonatal pigs. Biol Neonate 1999;76:33–43.
[10] Heilman KM, Gilmore RL. Cortical influences in emotion. J Clin Neurophysiol 1998;15:409–23.
[11] Henschen A, Lottspeich F, Brantl V, Teschemacher H. Novel opioid peptides derived from casein (beta-casomorphins). II. Structure of active components from bovine casein peptone. Hoppe-Seylers Z Physiol Chem 1979;360:1217–24.
[12] Leonard BE. The HPA and immune axis in stress: the involvement of the serotonergic system. Eur Psychiatry 2005;20(Suppl 3):S302–6.
[13] Luttinger D, King RA, Sheppard D, Strupp J, Nemeroff CB, Prange Jr AJ. The effect of neurotensin on food consumption in the rat. Eur J Pharmacol 1982;81:499–503.
[14] Mazella J, Botto JM, Guillemare E, Coppola T, Sarret P, Vincent JP. Structure, functional expression and cerebral localization of the levocabastine sensitive neurotensin/neuromedin N receptor from mouse brain. J Neurosci 1996;16:5613–20.
[15] Mazella J, Zsurger N, Navarro V, Chabry J, Kaghad M, Caput D, et al. The 100-kDa neurotensin receptor is gp95/sortilin, a non-G-protein-coupled receptor. J Biol Chem 1998;273:26273–6.
[16] Miclo L, Perrin E, Driou A, Papadopoulos V, Boujrad N, Vanderesse R, et al. Characterization of α-casozepine, a tryptic peptide from bovine α_{s1}-casein with benzodiazepine-like activity. FASEB J 2001;15:1780–2.
[17] Pettibone DJ, Hess JF, Hey PJ, Jacobson MA, Leviten M, Lis EV, et al. The effects of deleting the mouse neurotensin receptor NTR1 on central and peripheral responses to neurotensin. J Pharmacol Exp Ther 2002;300:305–13.
[18] Rowe W, Viau V, Meaney MJ, Quirion R. Stimulation of CRH-mediated ACTH secretion by central administration of neurotensin: evidence for the participation of the paraventricular nucleus. J Neuroendocrinol 1995;7:109–17.
[19] Sakaguchi M, Koseki M, Wakamatsu M, Matsumura E. Effects of systemic administration of beta-casomorphin-5 on learning and memory in mice. Eur J Pharmacol 2006;530:81–7.
[20] Sarret P, Beaudet A, Vincent JP, Mazella J. Regional and cellular distribution of low affinity neurotensin receptor mRNA in adult and developing mouse brain. J Comp Neurol 1998;394:344–56.
[21] Scruggs P, Filipeanu CM, Yang J, Chang JK, Dun NJ. Interaction of ovokinin(2–7) with vascular bradykinin 2 receptors. Regul Peptides 2004;120:85–91.
[22] Shibata K, Furukawa T. The mammillary body, a potential site of action of neurotensin in passive avoidance behavior in rats. Brain Res 1988;443:117–24.
[23] Shugalev NP, Khartmann G, Kertesh E. Aftereffects of microinjections of neurotensin into the substantia nigra of the brain on conditioned motor responses in rats with lesions to serotoninergic neurons. Neurosci Behav Physiol 2005;35:147–51.
[24] Sotrez-Bayon F, Cain CK, LeDoux JE. Brain mechanisms of fear extinction: historical perspectives on the contribution of prefrontal cortex. Biol Psychiatry 2005;60:329–36.
[25] Stiedl O, Palve M, Radulovic J, Birkenfeld K, Spiess J. Differential impairment of auditory and contextual fear conditioning by protein synthesis inhibition in C57BL/6N mice. Behav Neurosci 1999;113:496–506.
[26] Suzuki A, Josselyn SA, Frankland PW, Masushige S, Silva AJ, Kida S. Memory reconsolidation and extinction have distinct temporal and biochemical signatures. J Neurosci 2004;24:4787–95.
[27] Takahashi M, Fukunaga H, Kaneto H, Fukudome S, Yoshikawa M. Behavioral and pharmacological studies on gluten exorphin A5, a newly isolated bioactive food protein fragment, in mice. Jpn J Pharmacol 2000;84:259–65.
[28] Talukder MJ, Takeuchi T, Harada E. Receptor-mediated transport of lactoferrin into the cerebrospinal fluid via plasma in young calves. J Vet Med Sci 2003;65:957–64.
[29] Tanaka K, Masu M, Nakanishi S. Structure and functional expression of the cloned rat neurotensin receptor. Neuron 1990;4:847–54.
[30] Tsuji M, Takeda H, Matsumiya T. Different effects of 5-HT1A receptor agonists and benzodiazepine anxiolytics on the emotional state of naive and stressed mice: a study using the hole-board test. Psychopharmacology (Berl) 2000;152:157–66.
[31] Tyler-Mcmahon BM, Boules M, Richelson E. Neurotensin: peptide for the next millennium. Regul Peptides 2000;93:125–36.
[32] Vincent JP. Neurotensin receptors: binding properties, transduction pathways, and structure. Cell Mol Neurobiol 1995;15:501–12.
[33] Yamauchi R, Usui H, Yunden J, Takenaka Y, Tani F, Yoshikawa M. Characterization of β-lactotensin, a bioactive peptide derived from bovine β-lactoglobulin, as a

neurotensin agonist. Biosci Biotechnol Biochem 2003;67:940–3.
[34] Yamauchi R, Ohinata K, Yoshikawa M. β-Lactotensin and neurotensin rapidly reduce serum cholesterol via NT2 receptor. Peptides 2003;24:1955–61.
[35] Yamauchi R, Sonoda S, Jinsmaa Y, Yoshikawa M. Antinociception induced by β-lactotensin, a neurotensin agonist peptide derived from β-lactoglobulin, is mediated by NT_2 and D_1 receptors. Life Sci 2003;73: 1917–23.

Am J Physiol Regul Integr Comp Physiol 290: R449–R455, 2006.
First published September 22, 2005; doi:10.1152/ajpregu.00684.2004.

Dietary NaCl supplementation prevents muscle necrosis in a mouse model of Duchenne muscular dystrophy

Mizuko Yoshida,[1] Akira Yonetani,[2] Toshihiro Shirasaki,[2] and Keiji Wada[1]

[1]*Department of Degenerative Neurological Disease, National Institute of Neuroscience, National Center of Neurology and Psychiatry, Tokyo, Japan;* [2]*Hitachi High Technologies, Ibaraki, Japan*

Submitted 5 October 2004; accepted in final form 13 September 2005

Yoshida, Mizuko, Akira Yonetani, Toshihiro Shirasaki, and Keiji Wada. Dietary NaCl supplementation prevents muscle necrosis in a mouse model of Duchenne muscular dystrophy. *Am J Physiol Regul Integr Comp Physiol* 290: R449–R455, 2006. First published September 22, 2005; doi:10.1152/ajpregu.00684.2004.—The mdx mouse is an animal model for Duchenne muscular dystrophy. Mdx mice fed a 12% NaCl diet from birth up to 20 days of age (mdx-Na mice) had an ~50% reduction in serum creatine kinase (CK) activity compared with mdx mice fed a standard diet. Most notably, necrotic fibers in tibialis anterior (TA) muscle of mdx-Na mice were reduced by 99% and were similar in control mice. These mdx mice displayed significantly elevated blood Ca^{2+} and Na^+ levels, while the total calcium content of their TA muscle was reduced to the level of control mice. In addition, mdx-Na mice had elevated zinc and magnesium contents in their TA muscle. These results suggest that elevated serum Na^+ leads to Ca^{2+} extrusion from muscle via the Na^+/Ca^{2+} exchanger causing a decrease in intracellular Ca^{2+} levels and an increase in blood Ca^{2+} levels. Extracellular Ca^{2+} and, in addition, Zn^{2+} and Mg^{2+} might also contribute to the stabilization of the cell membrane. Other possibilities explaining the surprisingly efficacious beneficial effect of dietary sodium exist and are discussed.

therapy; calcium and zinc; potassium; blood; serum creatine kinase activity

DUCHENNE MUSCULAR DYSTROPHY (DMD), a severe X-linked recessive muscle-wasting disease, is a health problem with an incidence of 2–3 per 10,000 males in the world population (15). The disease is caused by a defect in the gene encoding dystrophin, a protein located on the inner surface of the plasma membrane (44). The exact function of dystrophin is unknown, and the prospects for successful treatment of DMD remain uncertain, although numerous studies of gene therapy for DMD (21, 22, 42, 43) and of pharmacological treatment (8, 17, 23, 33, 37, 40, 46) have been published.

In DMD patients and in mdx mice, an animal model of DMD, the disease is characterized by necrosis of muscle fibers that causes increased serum levels of the muscle enzymes creatine kinase (CK) and pyruvate kinase (32, 48).

Dystrophin-deficient muscle membranes allow excess Ca^{2+} influx, causing calcium accumulation in necrotic muscle fibers (6, 11). The total calcium content of skeletal muscle fibers in DMD patients (3, 4, 24, 29) and mdx mice (19, 30, 34) is higher than that found in normal muscle fibers. The causes leading to excess Ca^{2+} influx into dystrophin-deficient muscle fibers are still unclear, although the following mechanisms have been proposed: *1*) because dystrophin is thought to have a mechanical function, dystrophin-deficient muscle fiber membranes are predisposed to rupture (2, 10); *2*) Ca^{2+} leak channels or stretch-activated channels open more easily in dystrophic myotubes, leading to poor Ca^{2+} regulation (18); and *3*) the function of L-type Ca^{2+} channels is abnormal (12, 47).

We found earlier that serum CK activity in mdx females more than 60 days of age is less than 50% of that observed in males in agreement with published observations (38). Also, we previously found that mdx mice given saline from ages 7 to 24 days exhibit significantly reduced serum CK activity by day 25. These interesting findings led us to ask the following questions: *1*) How does saline decrease serum CK activity and, presumably, prevent muscle necrosis in mdx mice? *2*) Why is serum CK activity in mdx females lower in males? The answers to these questions may lead to effective therapies for halting the progression of DMD.

We hypothesize that *1*) saline may affect the concentration of some ions in the extracellular space (ECS), as well as in muscle fibers differently in mdx and control mice, and 2) these changes may be different between mdx female and male mice.

MATERIALS AND METHODS

Materials. Blood and tibialis anterior (TA) muscles of mice were used; mdx (C57BL/10ScSn-mdx) and control (C57BL/10ScSn; B10) mice were fed a standard diet (CE-2, Clea Japan, Tokyo, Japan) or a standard diet supplemented with 12% (wet wt) NaCl (NaCl diet). These mice are termed "mdx-Na" and "B10-Na." The diet containing 12% NaCl was given to pregnant mice beginning 2–3 days before delivery and continued throughout the life of the offspring. Thus NaCl passed from mothers to their offspring via milk until the pups were 20 days old. Some mice also consumed the NaCl diet directly as of about day 17.

Blood for measurement of serum CK activity and TA muscle for morphological analysis, as well as for determination of inorganic ion concentration and TA muscle fibers for metal elements, was collected from the same mouse. The number of mice used in this study is shown in the results. Our male and female B10, as well as mdx mice that were fed a standard diet (CE-2, Clea Japan), are able to produce offspring for 6 to 14 mo. Mouse experiments were performed in strict accordance with the guidelines of the National Institute of Neuroscience, National Center of Neurology and Psychiatry of Japan and were approved by the Animal Investigation Committee of the Institute.

Measurement of serum CK activity. The blood of mice (*day 7* to *90*) was withdrawn by inserting a syringe into the vena cava inferior of mice under deep ether anesthesia. The blood was then transferred to a 1.5-ml Eppendorf tube, allowed to stand for 2 h at room temperature, and centrifuged at 8,000 rpm using a TOMY MRX-150 centrifuge at

Address for reprint requests and other correspondence: Mizuko Yoshida, Department of Degenerative Neurological Disease, National Institute of Neuroscience, NCNP, 4-1-1 Ogawahigashi, Kodaira, Tokyo 187–8052, Japan (e-mail: yoshidam@ncnp.go.jp).

The costs of publication of this article were defrayed in part by the payment of page charges. The article must therefore be hereby marked "*advertisement*" in accordance with 18 U.S.C. Section 1734 solely to indicate this fact.

0363-6119/06 $8.00 Copyright © 2006 the American Physiological Society

Table 1. *Mice serum creatine kinase (CK) activity, blood K^+ and Ca^{2+} concentration in male and female mdx and B10 mice from days 7 to 90*

Age, days	Strain	Sex	CK activity × 10^3, U/l	K^+, mM	Ca^{2+}, mM
7	mdx	M	0.360±0.122 (n=28)[a]		
		F	0.347±0.107 (n=29)[b]		
		M + F		3.9±0.29 (n=31)[a]	1.51±0.0387 (n=31)
	B10	M	0.355±0.160 (n=32)		
		F	0.397±0.178 (n=26)		
		M + F		3.8±0.30 (n=29)	1.54±0.0695 (n=29)
20	mdx	M	7.80±4.58 (n=33)[c]		
		F	7.86±4.31 (n=33)[d]		
		M + F		4.9±0.44 (n=28)[b]	1.31±0.0417 (n=28)
	B10	M	0.235±0.0598 (n=37)[e]		
		F	0.244±0.0442 (n=33)[f]		
		M + F		3.7±0.30 (n=29)	1.30±0.0363 (n=29)
60	mdx	M	15.3±13.1 (n=32)[g]		1.23±0.0431 (n=31)[a]
		F	6.73±3.97 (n=33)[h]		1.25±0.0330 (n=32)
		M + F		5.0±0.47 (n=56)[h]	
	B10	M	0.105±0.0771 (n=23)		1.20±0.0334 (n=30)[b]
		F	0.051±0.0145 (n=28)		1.23±0.0344 (n=31)[c]
		M + F		3.6±0.31 (n=60)	
90	mdx	M	16.8±10.1 (n=33)[i]		1.17±0.0334 (n=27)[d]
		F	7.91±4.97 (n=32)[j]		1.19±0.0353 (n=30)[e]
		M + F		5.0±0.61 (n=58)[h]	
	B10	M	0.084±0.0500 (n=34)		1.17±0.0243 (n=30)[f]
		F	0.065±0.0542 (n=34)		1.20±0.0280 (n=29)[g]
		M + F		3.6±0.32 (n=59)[c]	

Values are presented as means ± SD. Mice were fed a standard diet. M, male; F, female; n, number of mice examined. CK activity (serum): a vs. c, b vs. d, c vs. e, d vs. f, g vs. h, i vs. j, $P < 0.001$; c vs. g, $P < 0.004$. K^+ concentration: a vs. b, b vs. c, $P < 0.001$. Ca^{2+} concentration: a vs. b, $P < 0.002$; b vs. c, $P < 0.001$; d vs. e, $P < 0.01$; f vs. g, $P < 0.001$.

4°C (Tomy Seiko, Japan). Serum CK activity was determined with a Cica liquid CK test (Kanto Chemical, Japan) using Synchron CX7 (Beckman Coulter, Fullerton, CA).

Measurement of K^+, Ca^{2+}, and Na^+ concentrations in blood. Blood was collected into 1-ml syringes without anticoagulants by heart puncture under ether anesthesia. The blood was placed immediately in an i-STAT cartridge ($EC6^+$) (i-STAT, Princeton, NJ). The measurement of Ca^{2+}, Na^+, and K^+ concentrations was performed within 2.5 min after drawing blood.

Measurement of total potassium, calcium, sodium, magnesium, and zinc contents in muscle and food. The muscle was excised under deep ether anesthesia. TA muscle or food was placed in Teflon tubes and digested with 0.5 ml of ultrapure HNO_3 (Kanto Chemical) at 100°C for 2 h. The samples were diluted to 10 ml with ultrapure water. Potassium, calcium, sodium, magnesium, and zinc contents were determined using inductively coupled plasma emission spectrometry (P-4010, Hitachi High-Technologies, Tokyo, Japan).

Morphological analyses of TA muscle tissue. TA muscles of mice at *day 20* were excised and frozen immediately in isopentane cooled in liquid nitrogen. Cryostat transverse sections were stained by Carrazi's hematoxylin and eosin Y (1% solution; Muto Pure Chemical, Tokyo, Japan). Necrotic areas of muscle fibers were identified as described (6, 16) and analyzed with a Color Image Analyzer (SP-500 Olympus Optical, Tokyo, Japan). Necrotic areas correspond to the whole TA muscle area minus the white color area and normal (peripherally nucleated) fibers.

Statistics. Data are expressed as means ± SE or ± SD. The data were analyzed using the two-tailed Student's t-test.

RESULTS

Critical starting point of muscle fiber degeneration and differences between adult males and females. At the start of the study of the effect of NaCl on the degeneration of mdx muscle fibers, we decided to inhibit mdx muscle degeneration before the onset of muscle fiber necrosis. As shown in Table 1, the serum CK activity and blood K^+ concentration of mdx mice at *day 7* were similar to those of control B10 mice. Average serum CK activity and blood K^+ concentration in mdx mice began to increase only after *day 7*, and the K^+ concentration at *day 8* (*day 8*: 4.2 ± 0.1 mM, $P < 0.02$) and CK activity at *day 10* (*day 10*: 499 ± 28 U/l, $P < 0.001$) were significantly different from those at *day 7*. Serum CK activity and blood K^+ concentration also were significantly different for mdx mice between *days 7* and *20* ($P < 0.001$; Table 1). The results shown in Table 1 show that the serum CK activity and the K^+ concentration in blood of mdx mice began to increase after *day 7* compared with those of B10 mice, suggesting that the mdx cell membrane started to rupture after *day 7*, causing the CK and the K^+ to leak from muscle fibers to ECS. On the basis of these results, we started NaCl administration before *day 7*.

Blood Ca^{2+} concentration of both mdx and B10 female mice at *day 90* was significantly higher than that of males (Table 1). Although the differences of Ca^{2+} concentration between female and male mdx and B10 mice were small, the differences may be advantageous for the discussion, since blood Ca^{2+} concentration is strictly controlled (36). Serum CK activity of female mdx mice was about half of males' serum CK activity, as described in the introduction (Table 1). The values for serum CK activity in adult mdx mice are consistent with those reported by Suh et al. (38) and Takagi et al. (40).

Female TA muscle zinc contents of mdx and B10 mice were significantly higher than those in males of mdx and B10 mice. Muscle Zn content of mdx males was markedly higher than that of B10 males (Table 2).

Table 2. *Total zinc content in the tibialis anterior muscle of mdx and B10 male and female mice on day 60*

Sex	mdx	B10
M	13.7±0.216[a] (*n*=30)	12.2±0.216[c] (*n*=30)
F	14.8±0.272[b] (*n*=28)	15.7±0.339[d] (*n*=30)

Values are means ± SE. Zinc content is given in mg/kg wet weight. Mice were fed a standard diet. a vs. b, $P < 0.005$; c vs. d, a vs. c, $P < 0.001$; b vs. d, $P < 0.04$.

Effect of NaCl ingestion on serum CK activity and on morphology of mdx mice. We preliminarily examined whether a diet containing 1, 3, and 5% Na weight/weight (wt/wt) fed to mothers reduced serum CK activity of the offspring. Although 1 and 3% Na was insufficient, the diets containing 5% Na (In the following expression, a diet with 12% NaCl was used.) effectively reduced serum CK of mdx mice at *day 20* (Fig. 1). Therefore, these conditions were used in this study. The effect of NaCl ingestion on serum CK activity of mdx on *day 20* is shown in Fig. 1. The activity of this marker enzyme of muscle fiber degeneration was reduced to about 60% of that of mdx mice fed control food.

TA muscle fibers of mdx mice showed variations in fiber size, shape, and the incidence of large, dark fibers, and necrotic fibers were increased (Fig. 2, mdx). In contrast, the TA muscle fibers of mice whose mothers ate a diet with elevated NaCl were nearly normal in appearance (Fig. 2, mdx-Na). The area of necrosis in TA muscle sections from mdx-Na mice was drastically lowered (0.46% of total area, $n = 12$) compared with mdx mice (46%, $n = 17$) ($P < 0.001$). In addition, sections from the mdx-Na mice showed a nearly normal muscle pattern.

Effect of NaCl ingestion on blood K^+, Ca^{2+}, and Na^+ concentrations. The effect of NaCl ingestion (via mothers' milk) on blood K^+ and Ca^{2+} concentration of mdx-Na and control mice is shown in Fig. 3. Although NaCl had no effect on blood K^+ concentration in control mice, this ion was 11% lower in mdx-Na than in mdx mice ($P < 0.001$; Fig. 3*A*).

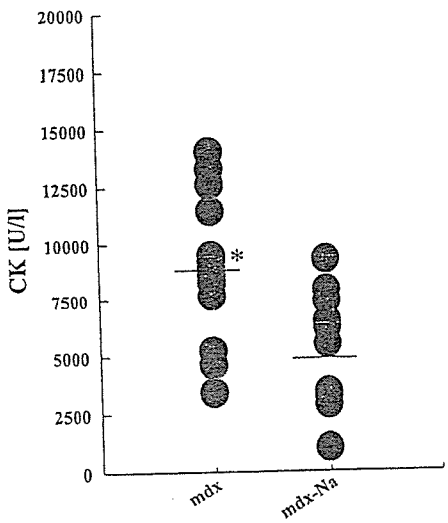

Fig. 1. Effect of NaCl ingestion on serum CK activity in mdx-Na mice at day 20. Mdx mice ($n = 16$) were fed a standard diet. Mdx-Na ($n = 13$) mice were fed a diet containing 12% NaCl (wt/wt); *$P < 0.001$. Horizontal lines indicate mean values.

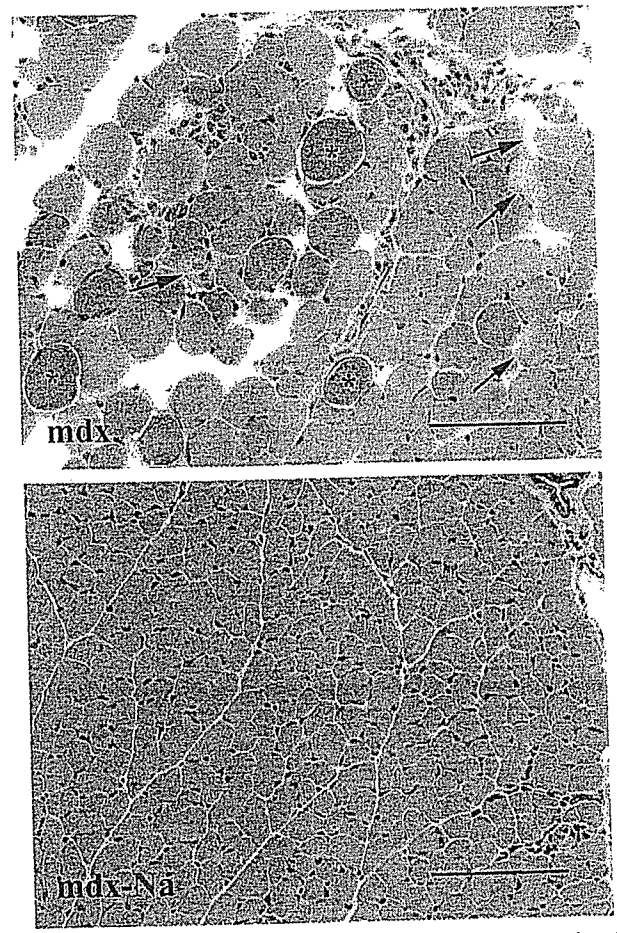

Fig. 2. Tibialis anterior muscle fibers from 20-day-old mdx mice fed a standard diet (mdx) and mdx-Na mice fed a diet containing 12% NaCl (mdx-Na). Muscle fibers from the mdx mouse show size variation, round shape, and large dark fibers (*), as well as necrotic fibers (arrows). Scale bars indicate 100 μm.

Blood Ca^{2+} and Na^+ levels in mdx-Na and control mice were significantly elevated compared with those on the control diet (Ca^{2+}: Fig. 3*B*, Na^+: data not shown).

Effect of NaCl ingestion on calcium, sodium, potassium, magnesium, and zinc content in TA muscle. The calcium and sodium content of TA muscles from mdx mice were markedly higher than those from B10 mice (Fig. 4, Ca and Na). NaCl administration significantly increased B10-Na muscle calcium ($P < 0.02$) and Na contents ($P < 0.001$). However, muscle calcium and sodium contents of mdx-Na mice were dramatically lower than those of mdx mice (both $P < 0.001$) and close to the levels in B10-Na mice.

Muscle potassium and magnesium contents in mdx mice were significantly lower compared with B10 mice (both $P < 0.001$; Fig. 4, K and Mg). In mdx-Na mice, muscle potassium and magnesium contents were noticeably higher as a result of NaCl supplementation (both $P < 0.001$).

The zinc content of muscle from mdx mice was significantly lower than that of the B10 controls ($P < 0.001$; Fig. 4, Zn). NaCl administration markedly elevated the muscle zinc content of both mdx-Na and B10-Na mice (both $P < 0.001$). Muscle Zn content of mdx-Na mice was close to that of B10 mice, but the difference was significant ($P < 0.01$).

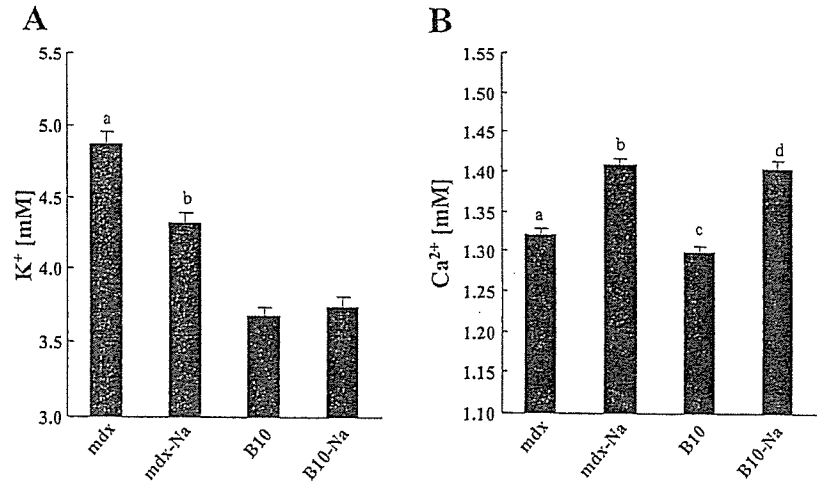

Fig. 3. Effect of NaCl ingestion on blood K^+ and Ca^{2+} concentration in mdx-Na and in B10-Na mice at day 20. *A:* K^+ concentration; mdx (n = 28) and B10 (n = 28) were fed a standard diet, mdx-Na (n = 29) and B10-Na (n = 29) were fed a diet containing 12% NaCl. a vs. b, $P < 0.001$. *B:* Ca^{2+} concentration; mdx (n = 27), mdx-Na (n = 28), B10 (n = 30), and B10-Na (n = 31), a vs. b, c vs. d, $P < 0.001$. Bars are mean, and vertical lines are SE.

DISCUSSION

We found earlier that mdx mice given saline by injection exhibited significantly reduced serum CK activity. We have now investigated whether oral supplementation of NaCl reduced serum CK activity and inhibited mdx muscle degeneration if given before the onset of muscle fiber necrosis.

Results in Table 1 show that the serum CK activity and the K^+ concentration in the blood of mdx mice began to increase after *day 7* compared with those of B10 mice, suggesting that the mdx cell membrane started to rupture after *day 7*, causing the CK and the K^+ to leak from muscle fibers into ECS. On the basis of these results, we started NaCl administration before *day 7*. NaCl-supplement administration significantly reduced muscle fiber degeneration of mdx mice at *day 20* (Figs. 1 and 2). NaCl administration also reduced blood K^+ concentration (Fig. 3*A*) and muscle sodium content (Fig. 4, Na), and increased potassium and magnesium in muscle fibers in mdx-Na mice (Fig. 4, K and Mg). The muscle calcium content of mdx-Na mice decreased drastically compared with that of mdx mice (Fig. 4, Ca) and close to the levels in B10-Na mice. The 99% decrease in the area of necrotic fibers in mdx-Na mice shows that NaCl supplementation almost completely inhibits mdx TA muscle fiber necrosis (Fig. 2). In mdx-Na and B10-Na mice, blood Na^+ and Ca^{2+} concentrations (Ca^{2+}: Fig. 3*B*) and muscle zinc content (Fig. 4, Zn) increased on *day 20* relative to the control. It is unknown why NaCl administration increased both zinc content in muscle fibers and blood Ca^{2+} concentration concurrently.

These results may have important implications for the inhibition of muscle necrosis, as Ca^{2+}, Na^+ and Zn^{2+} play critical physiological roles. We expect that the process of muscle degeneration in DMD or mdx mice causes excess Ca^{2+} to accumulate gradually in fibers after reaching a critical point in time, because their muscle fibers appear to function normally until a critical period is reached (47). In the case of mdx mice, the serum CK activity and K^+ concentration do not increase until around age 7 days (Table 1). When muscle fibers, with high levels of accumulated calcium, receive stimulation, the fibers subsequently undergo extreme hypercontraction at the critical point (after age 7 days) and may lead to membrane rupture (47). At this moment, K^+ may leak into the ECS and might produce the contraction of other muscle fibers around the ruptured fibers [potassium-induced contracture (27)].

We believe that group necrosis of muscle fibers following the efflux of K^+ may be one of the causes of necrosis of muscle fibers, in addition to the "theories on grouped necrosis" described by Gorospe et al. (20). The TA muscles of mdx-Na mice did not show group necrosis except in one case. Aside from the Ca^{2+}-stabilizing effect, reduced serum CK activity, blood K^+ concentration, and the group necrosis fibers of mdx-Na mice may have been caused by a quick, excessive K^+ excretion with excessive Na^+ excretion in urine, as the urinary potassium excretion rate depends on urinary volume (35). The mice that ingested the Na supplement drank excessive water and evacuated a large amount of urine, although we do not have data on the volume of their urine. Atrial natriuretic peptide (ANP) in the blood of the mice that ingested the Na supplement might have increased, since the high-salt diet induces an increase in ANP plasma levels (28). ANP has been also known to block sarcolemmal L-type Ca^{2+} channel activity and the Ca^{2+} release from the sarcoplasmic reticulum (SR) (25). The L-type Ca^{2+} channels and the Ca^{2+} release from the SR in mdx-Na muscle fibers may have been inhibited by the ANP, which prevents calcium accumulation in mdx-Na muscle fibers.

Mouse skeletal muscle fibers possess a Na^+/Ca^{2+} exchange mechanism (1). High Na^+ levels in the ECS serve to force efflux of Ca^{2+} from fibers via the Ca^{2+}/Na^+ exchanger and inhibit Ca^{2+} release from the SR (13). The average blood Na^+ concentration in mdx-Na and B10-Na mice was significantly elevated. Thus the Na^+/Ca^{2+} exchanger of mdx-Na muscle fibers may have prevented calcium accumulation in mdx-Na muscle fibers and might contribute to increase Ca^{2+} concentration in blood (and ECS).

Lijnen and Petrov (26) demonstrated reduction of the total calcium content of erythrocytes and the intraplatelet Ca^{2+} concentration by calcium supplementation. The mean value of serum Ca^{2+} concentration and the plasma total calcium content of the treated calcium group was higher than in the placebo group, although there are no significant differences between the calcium and placebo groups. They also showed a reduction in the plasma concentrations of intact parathormone and 1,25-dihydroxyvitamin D3 that raise calcium uptake in cells (7, 9). Increased Ca^{2+} concentration in the blood of mdx-Na might have been produced to reduce the activity of parathormone and

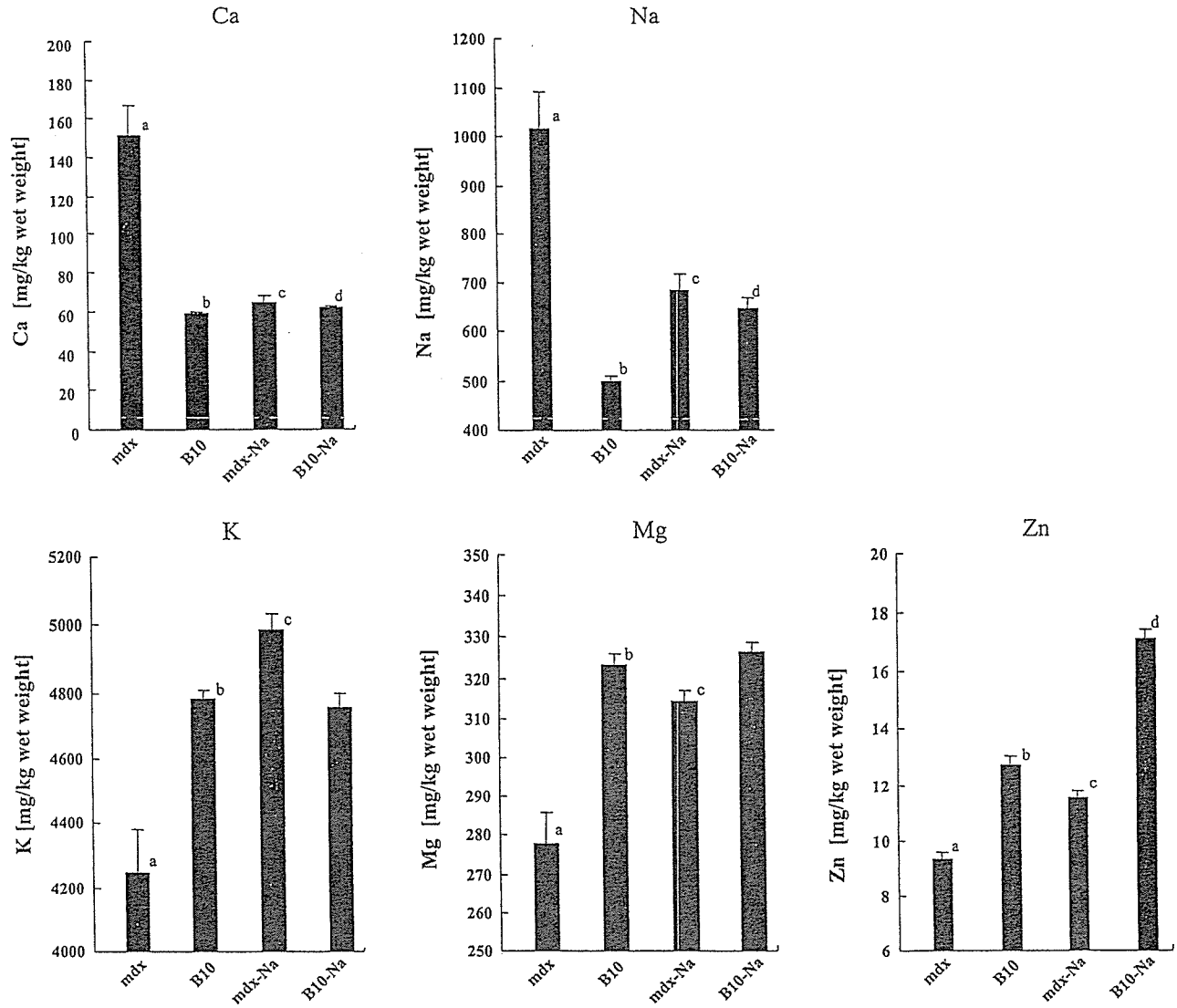

Fig. 4. Effect of NaCl ingestion on total calcium, sodium, potassium, magnesium, and zinc content in the tibialis anterior muscle of mdx-Na and B10-Na mice at *day 20*. Mdx and B10 were fed a standard diet; mdx-Na and B10-Na were fed a diet containing 12% NaCl. Ca, calcium content; mdx (n = 29), B10 (n = 31), mdx-Na (n = 25) and B10-Na (n = 27); a vs. b, a vs. c, $P < 0.001$; b vs. d, $P < 0.02$. Na: sodium content; mdx (n = 29), B10 (n = 31), mdx-Na (n = 25), and B10-Na (n = 27); a vs. b, a vs. c, b vs. d, $P < 0.001$. K: potassium content: mdx (n = 30), B10 (n = 31), mdx-Na (n = 25) and B10-Na (n = 27). a vs. b, a vs. c, $P < 0.001$. Mg: magnesium content; mdx (n = 29), B10 (n = 31), mdx-Na (n = 25) and B10-Na (n = 30); a vs. b, a vs. c, $P < 0.001$. Zn: zinc content; mdx (n = 30) and B10 (n = 31), mdx-Na (n = 27) and B10-Na (n = 30); a vs. b, a vs. c, b vs. d, $P < 0.001$. Bars are means, and vertical lines are SE.

1,25-dihydroxyvitamin D3 and may have prevented calcium accumulation in muscle fibers of mdx mice.

Activation of Ca^{2+}-ATPase of erythrocytes by calcium supplementation (49) and high activity of Ca^{2+}-ATPase in dystrophic muscle sarcolemma (14, 39) were demonstrated. High Ca^{2+} concentration in the blood of mdx-Na mice may have induced Ca^{2+}-ATPase to higher activity for the prevention of Ca^{2+} accumulation in muscle fibers and might have protected them from calcium accumulation in muscle fibers of mdx mice. From the above discussions, it is conceivable that higher Ca^{2+} in the blood (or in ECS) of female mdx mice reduced the calcium accumulation in their muscle fibers, inhibited necrosis of muscle fibers, and stabilized membrane effects of Ca^{2+}.

The zinc content of TA muscle of mdx-Na or female mdx mice was higher than that of muscle of mdx mice fed a control diet or of male mdx mice. Zinc may be important to inhibit muscle necrosis because Zn^{2+} stabilizes cell membranes (5) and blocks L-type Ca^{2+} channels (45). One of the reasons why serum CK activity in mdx females is lower than in males may be higher zinc content of muscle than that of muscle of males. Muscle zinc content of mdx males was markedly higher than that of B10 males (Table 2). These results suggest the importance of zinc in mdx mice surviving as long as control B10 mice. Mdx males seem to require higher muscle zinc content to survive as long as B10 mice. Zn^{2+} also plays a role in protein synthesis and may contribute to the regeneration of muscle fibers. Therefore, Zn^{2+} may be important for muscle regeneration in mdx mice. The assumption is supported by the results of Tameyasu et al. (41), which suggest that the administration of a zinc compound ameliorates muscle function in the mdx